



2333-31

Workshop on Science Applications of GNSS in Developing Countries (11-27 April), followed by the: Seminar on Development and Use of the Ionospheric NeQuick Model (30 April-1 May)

11 April - 1 May, 2012

GPS Observations of Plasma Bubbles and Scintillations over Equatorial Africa

VALLADARES Cesar
Institute for Scientific Research, Boston College
St. Clement's Hall
140 Commonwealth Avenue
CHESTNUT HILL MA 02467-3862
Massachusetts
U.S.A.

GPS OBSERVATIONS OF PLASMA BUBBLES AND SCINTILLATIONS OVER EQUATORIAL AFRICA

Vadym Paznukhov¹, Charles S. Carrano¹, Keith M. Groves², Ronald G. Caton², Cesar E. Valladares¹, Gopi K. Semala¹, Christopher T. Bridgwood¹, Jacob Adeniyi³, Larry L. N. Amaeshi⁴, Baylie Damtie⁵, Florence **D'Ujanga** Mutonyi⁶, Jared O. H. Ndeda⁷, Paul Baki⁸, Olivier K Obrou⁹, Bonaventure Okere¹⁰, Gizaw Mengistu Tsidu¹¹

1. Institute for Scientific Research, Boston College

2. AirForce Research Laboratory, Hanscom Field, MA

3. University of Ilorin, Ilorin, Nigeria

4. University of Lagos, Lagos, Nigeria

5. Bahir Dar University, Bahir Dar, Ethiopia

6. Makerere University, Kampala, Uganda

7. Jomo Kenyatta University, Nairobi, Kenya

8. University of Nairobi, Nairobi, Kenya

9. Université de Cocody à Abidjan, Abidjan, Cote d'Ivoire

10. University of Nigeria, Nsukka, Nigeria

11. Addis Ababa University, Addis Ababa, Ethiopia



Outline



Introduction

Review of the physics of equatorial plasma bubbles. Seeding mechanisms.

- Early observations
- Satellite and radar observations
- Gravity wave seeding, Pre-reversal enhancement and the sunset vortex (wind driven gradients drift instability).
- Large scale wave structures (LSWS)

Observation of TEC depletions in South America

SCINDA ground stations in Africa. Comparison of GPS scintillations in the Atlantic, West and East sectors.

Automatic detection of TEC depletions. Comparison to previous satellite observations.

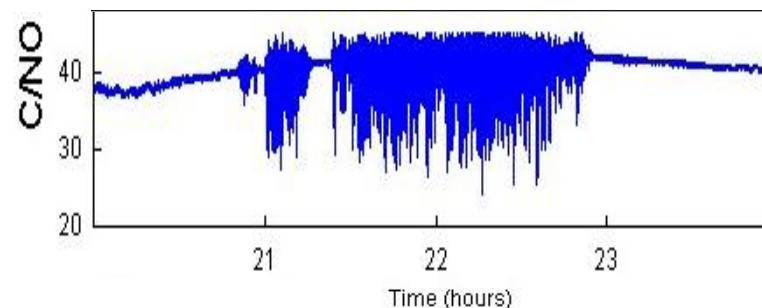


Introduction



- Equatorial Plasma Bubbles (EPB) are irregular plasma density depletions observed by satellites and radar backscatter in the equatorial F-region ionosphere. Their dynamics follow the generalized (nonlinear) Rayleigh-Taylor (R-T) instability in the bottomside of the F layer. Inside EPBs the bottomside plasma interchanges with plasma near and above the F layer peak.
- Scintillations are rapid amplitude and phase fluctuations of radio signals from space due to forward-scatter from ionospheric irregularities. At L band, they are usually caused by EPB (as opposed to bottom-type or other irregularities which can affect lower frequency systems, e.g. VHF).

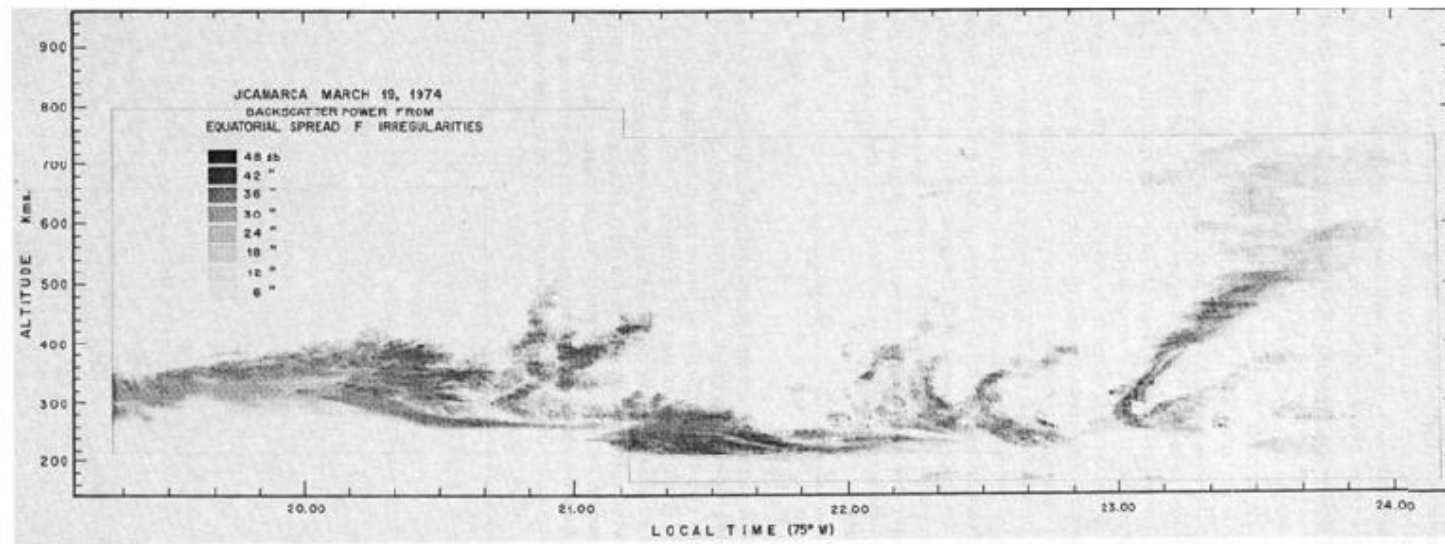
Scintillated GPS Signal



- The climatology of GPS scintillations in Africa are not well established due to a scarcity of ground-based observations. We compare the climatology of EPB and scintillation observed using networks of GPS receivers in Africa.

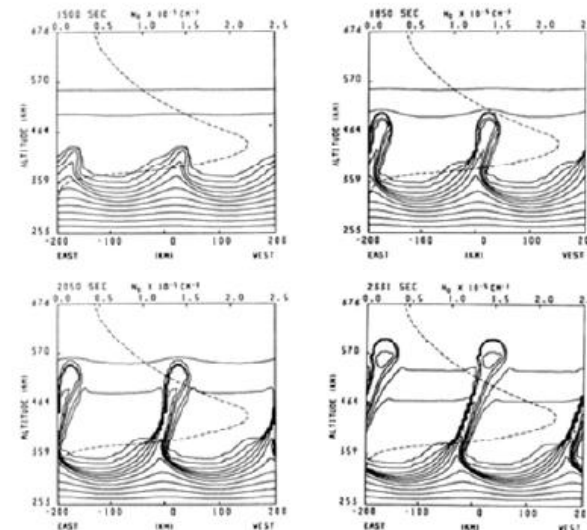
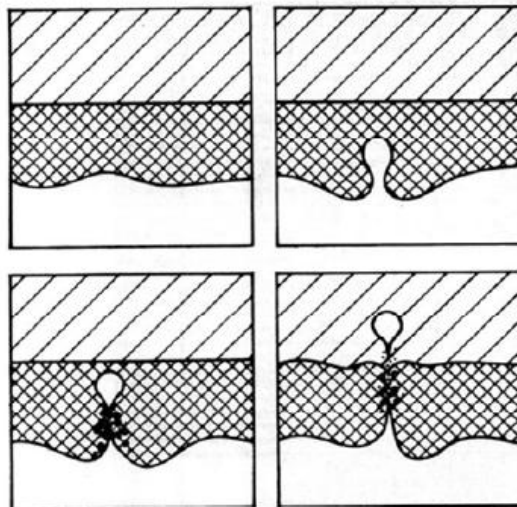


Radar plumes measured by the Jicamarca radar (70's)



Woodman and LaHoz, 1976

Sketch of how the low density bubble propagates to the stable topside.



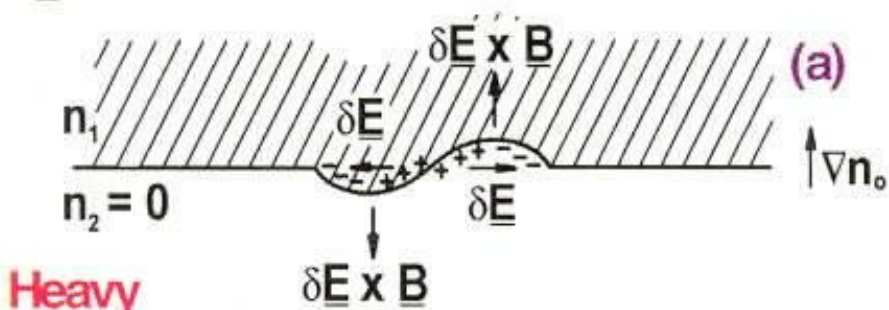
Numerical simulation of Rayleigh-Taylor in the non-linear regimen. Zalesak et al., 1982.



Rayleigh-Taylor Instability

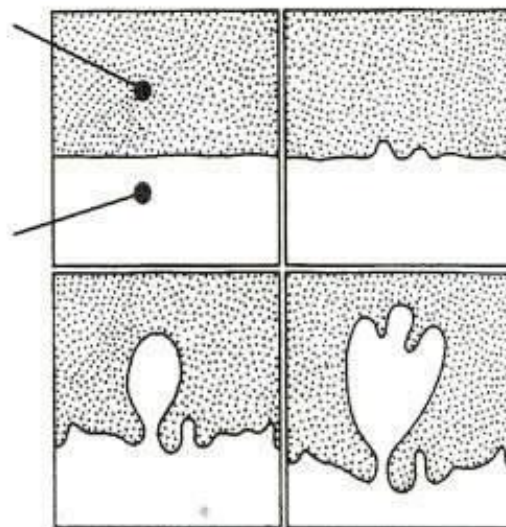


$$\underline{B} \rightarrow \underline{J} = \frac{nMg \times \underline{B}}{B^2} \quad \underline{B} \otimes \underline{E}_o \text{ and } \underline{J} = \sigma_p \underline{E}_o$$



Heavy Fluid

Light Fluid



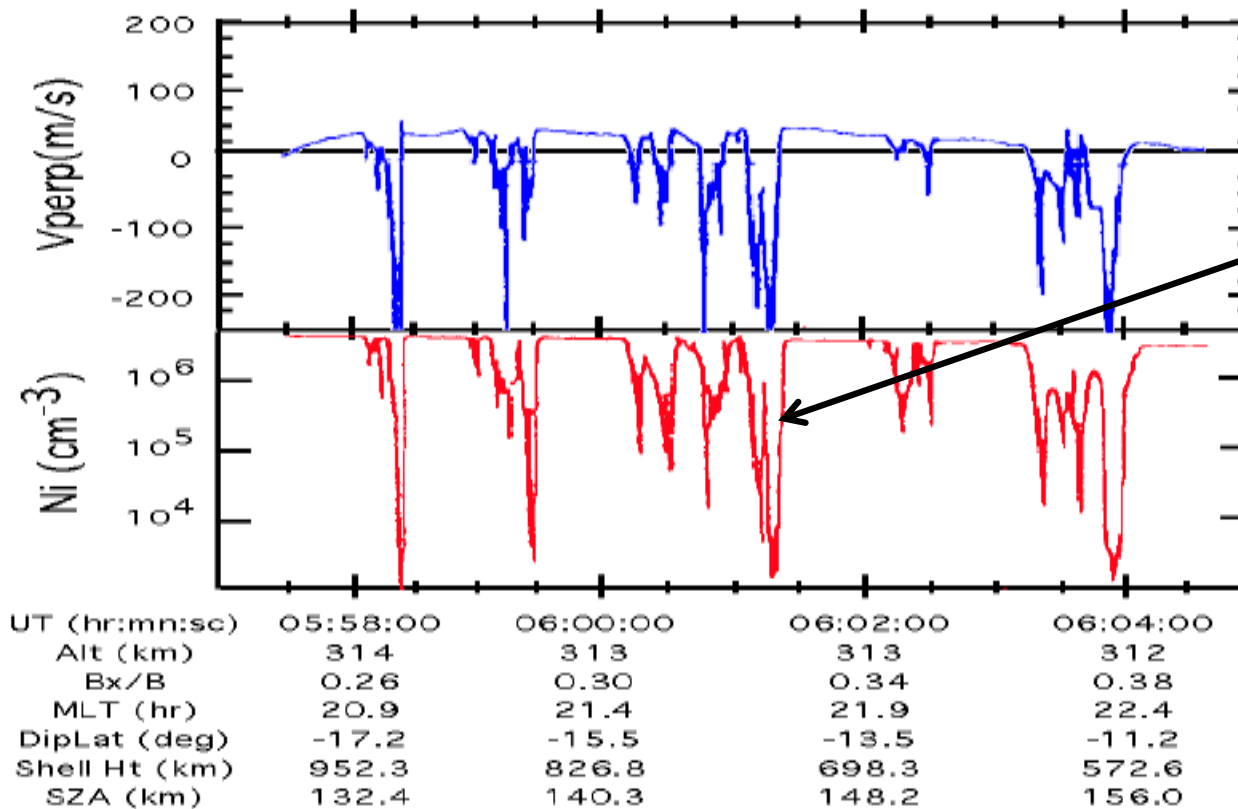
R-T Growth Rate

$$\gamma = \frac{\sum_P^F}{\sum_P^E + \sum_P^F} \left(V_p + U_n^P + \frac{g_L}{v_{in}^{eff}} \right) \frac{1}{L_n} - R_T$$

(a) Schematic diagram of the plasma analog of the hydrodynamic R-T instability in the equatorial geometry. (b) Sequential sketches from photos of the hydrodynamic R-T instability. A lighter fluid initially supports a heavy fluid.



Atmospheric Explorer-E Plasma Bubbles



Plasma depletions associated with bubbles

Upward ion velocity in some bubbles increase approximately with δN reaching a limit much larger than the value predicted by R-T instability. These values may result from a seed.

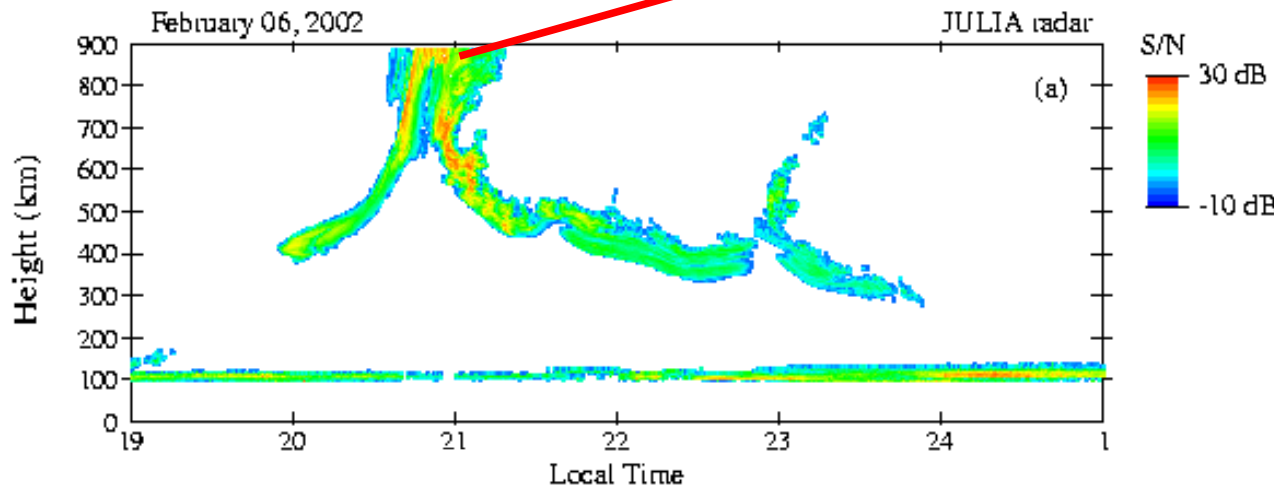
Hanson and Bamgboye, JGR, 8997, 1984



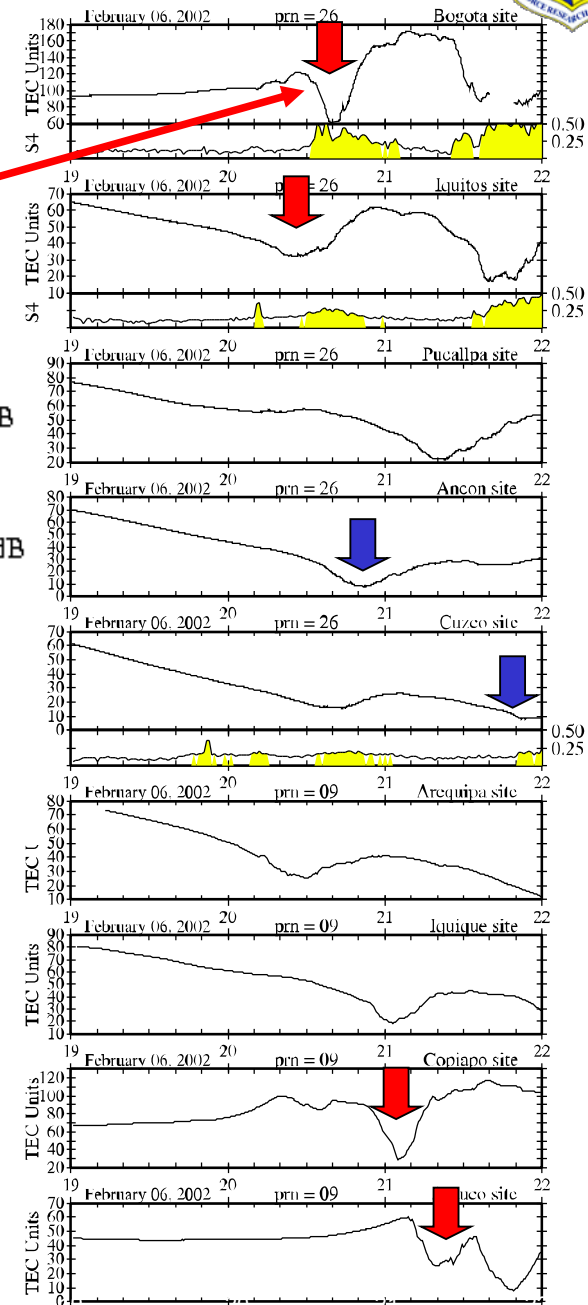
Radar plume associated with TEC depletions Feb 06, 2002



Due to the plume's westward tilt the TEC depletion is seen first at Iquitos (8 N) and then at Bogota (16°N).

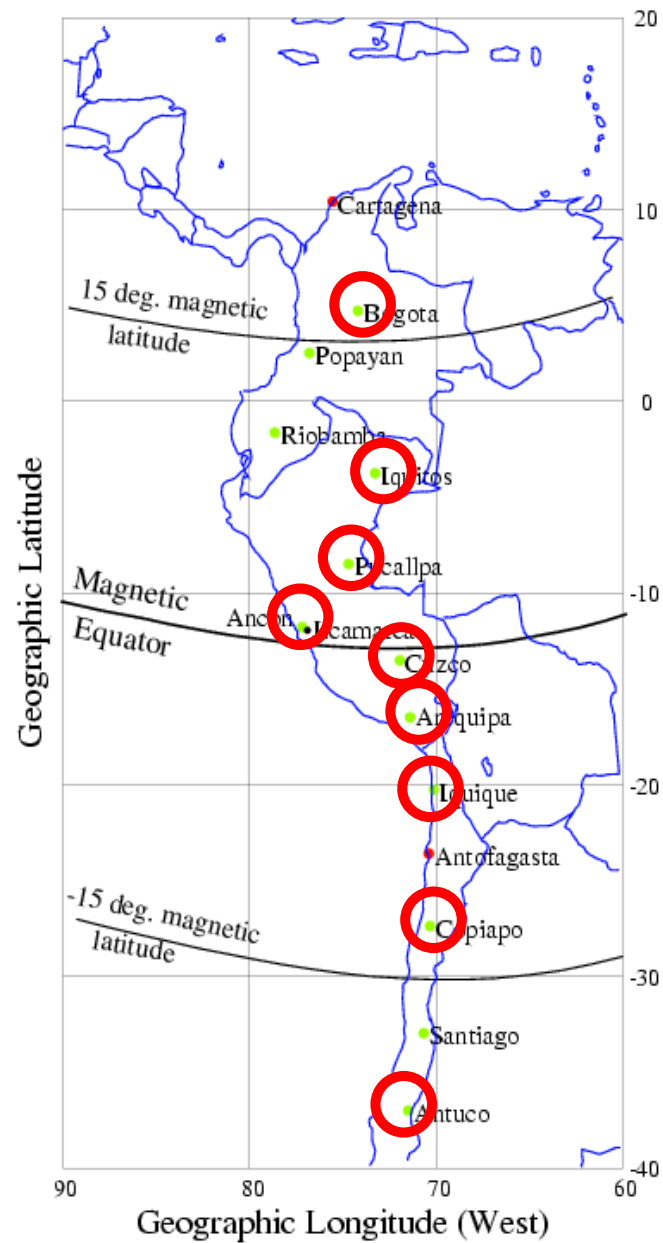


Near the magnetic equator the TEC depletions are only 20 TECU (blue arrows). Near the crests they are about 50 TECU (red arrows).





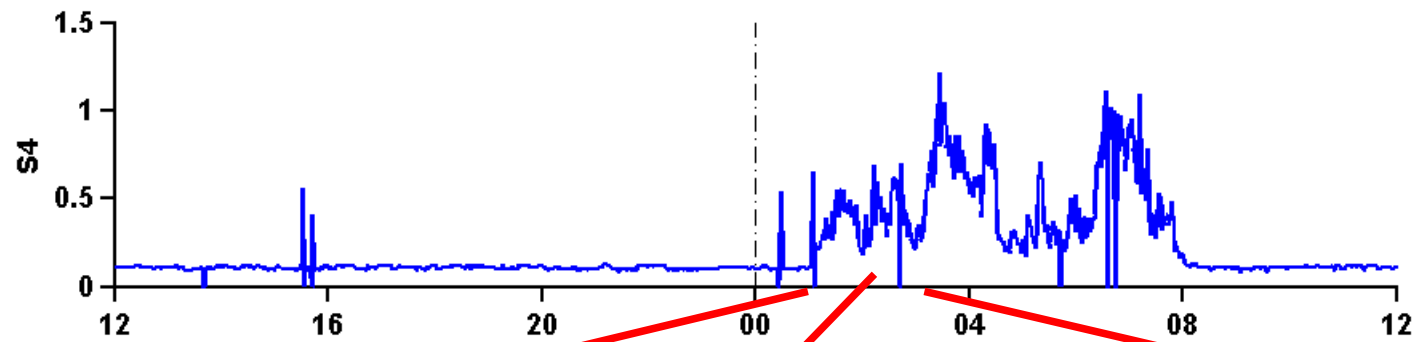
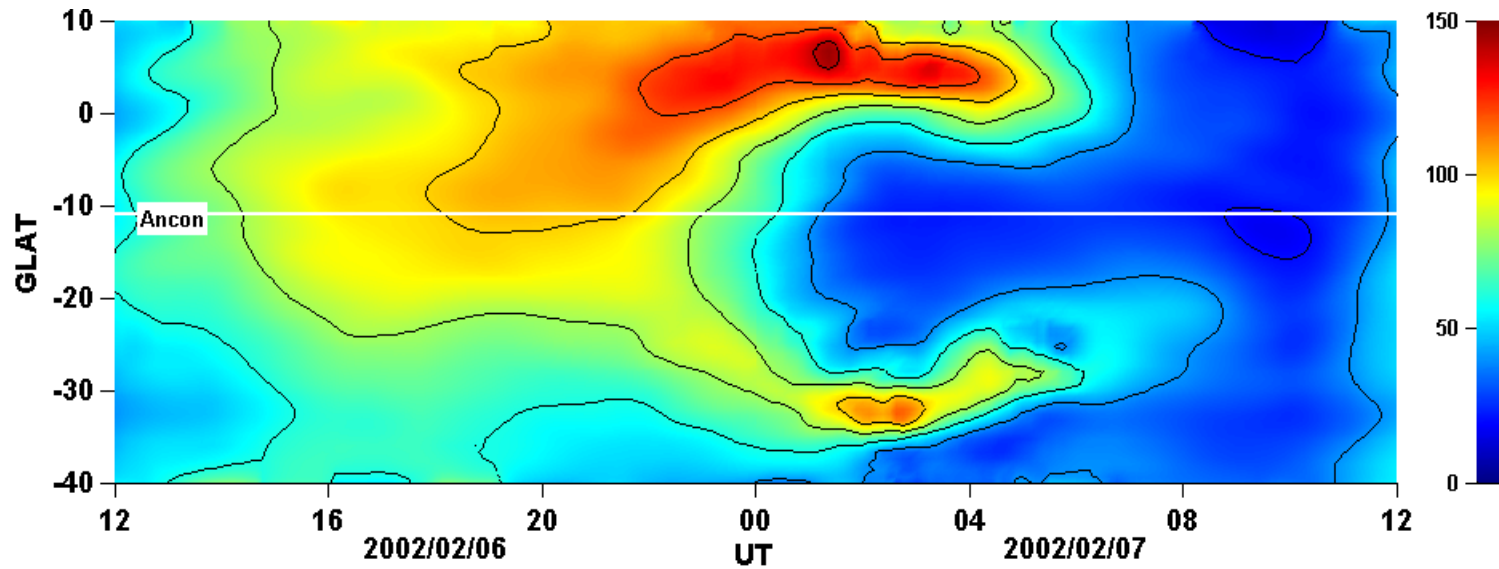
Depletions Recorded by the South American Chain of Stations



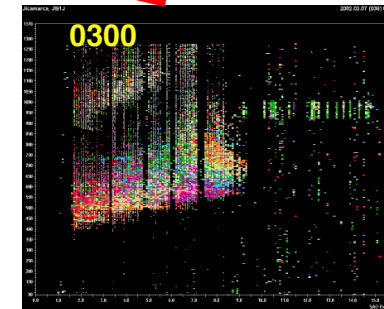
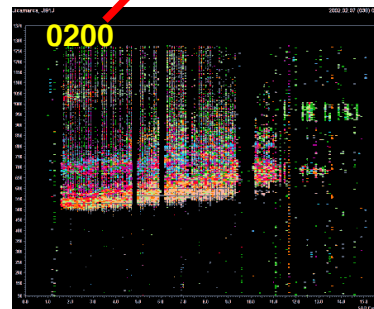
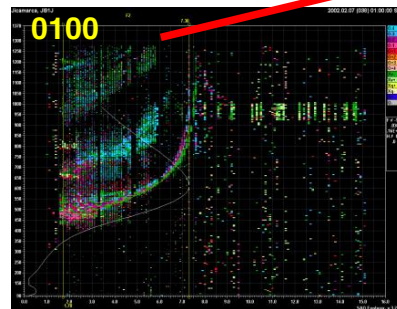


TEC, UHF Scintillations, and Ionograms

Feb 07, 2002

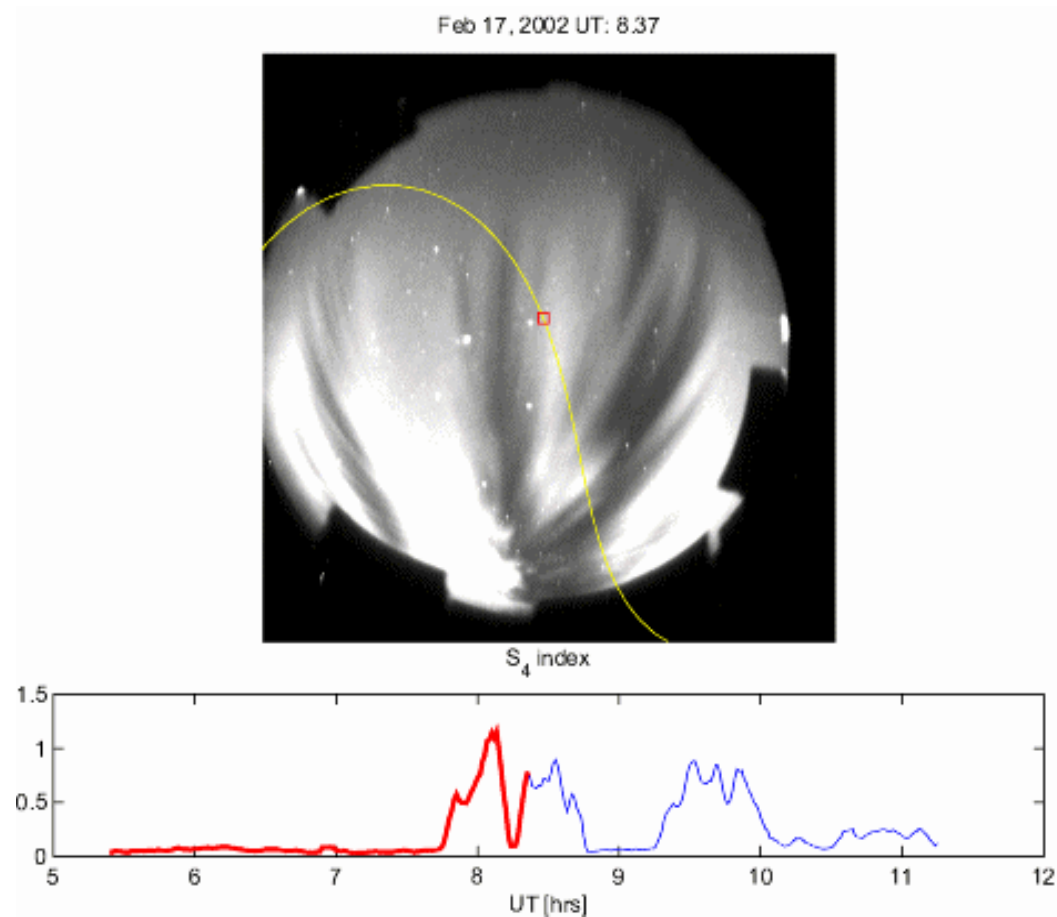


Jicamarca
sounder
observes
range-type
ionograms





Airglow depletions using 777.4 nm emissions



Haleakala all-sky camera (ASC) image and GPS scintillations. Severe scintillations, as shown in the lower panel by the S_4 index from the GPS data, correlate to depleted regions of electron density (upper panel).

Makela et al., GRL, 2004

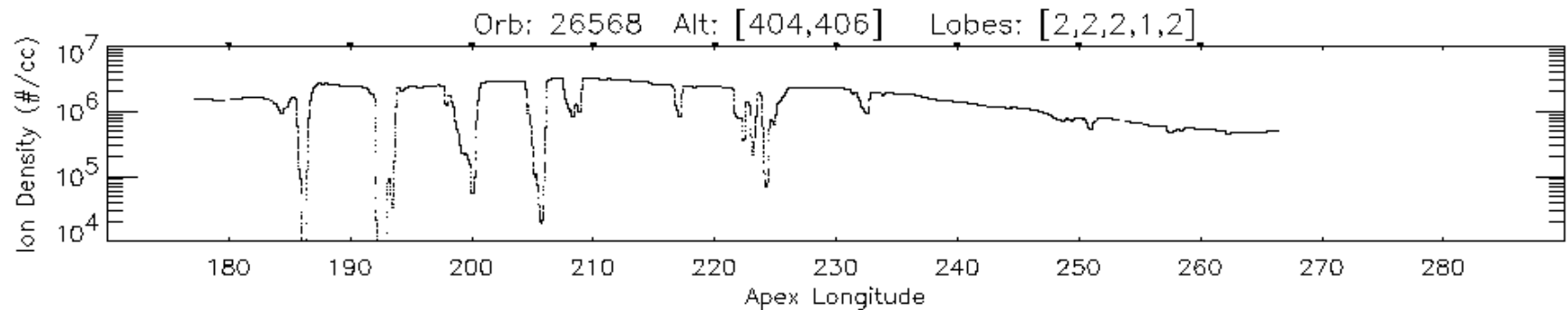


Plasma Bubbles Observed by AE-E

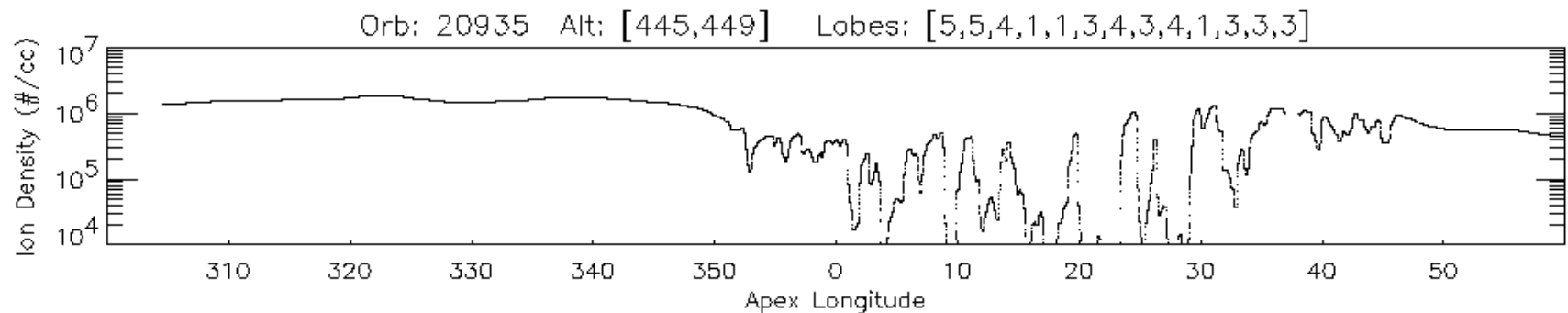


- Pacific Depletions most often appear as bubble groups about 500 km wide in a background that is quite uniform.
- **Africa depletions appear as bubble groups in excess of 1000 km wide in a background that has a large-scale depression.**

Pacific:



Africa:



Hei, et al., (2005) seasonal and longitudinal variation of large-scale topside equatorial plasma depletions JGR.



Seeds, why we need seeds?



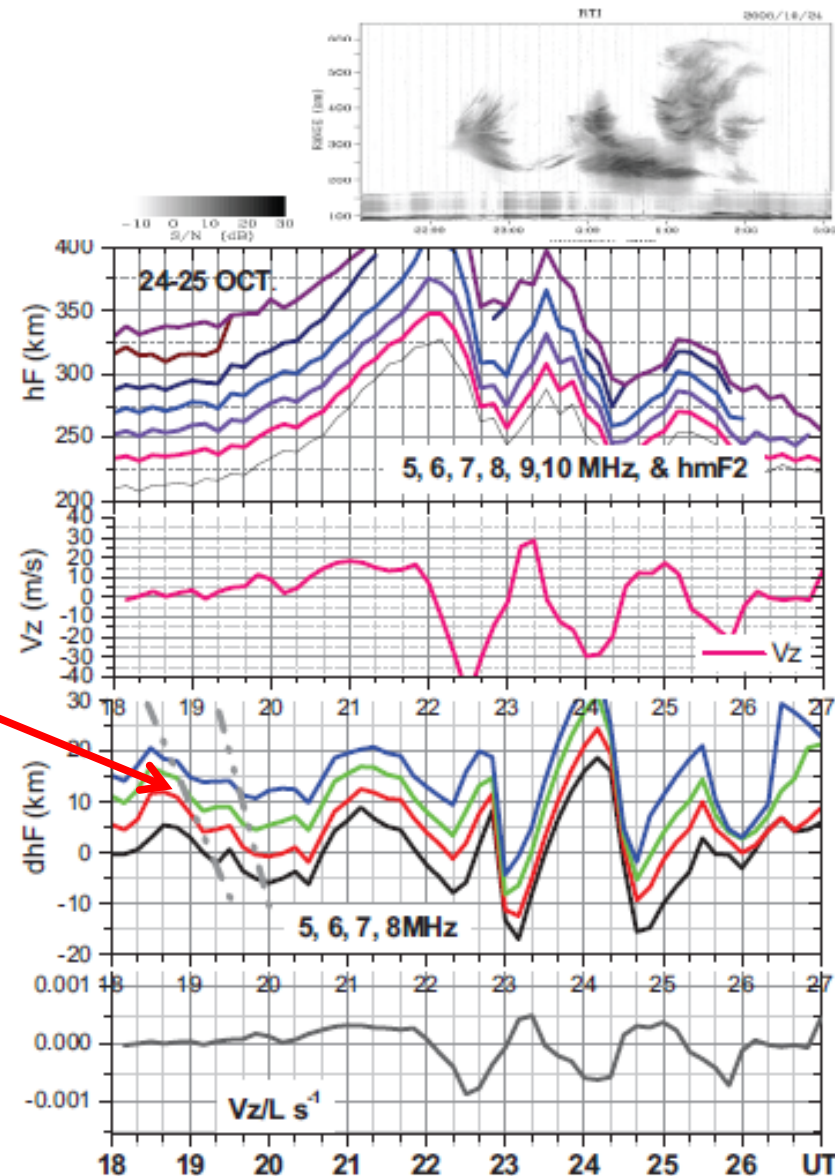
The calculated RTI growth rate for the evening ionosphere generally has an e-folding time of 15 minutes or greater. This is too slow for the observed rapid development of plasma plumes after sunset.

Atmospheric gravity waves can modulate the atmosphere through wind and electric field spatial variations that act as seeds of plasma bubbles [*Huang and Kelley, 1996*].

Seeds influence occurrence and properties of topside plasma structures. They may explain why the bubbles are highly depleted and densely packed in Africa instead of less depleted and widely spaced clusters in the Pacific sector [*Hei et al., 2005*].



Experimental evidence of Gravity waves with phase velocity propagating downward.

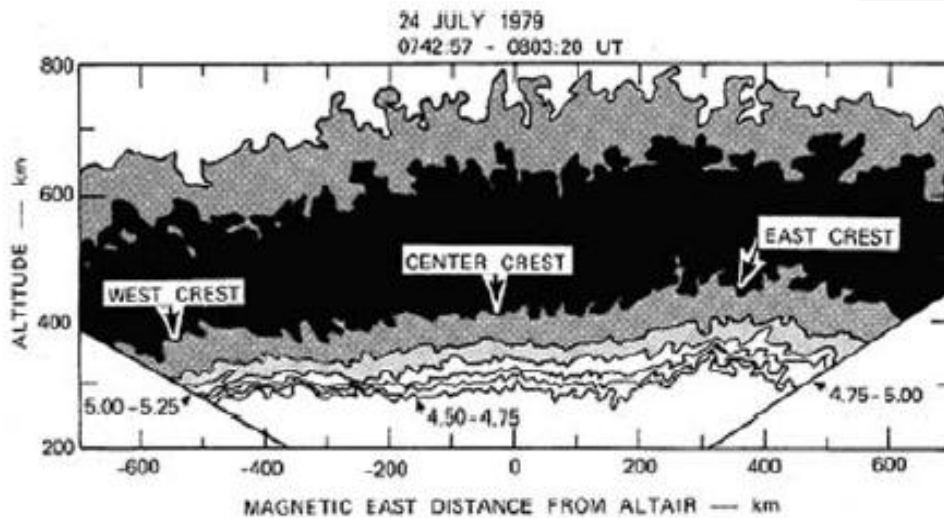
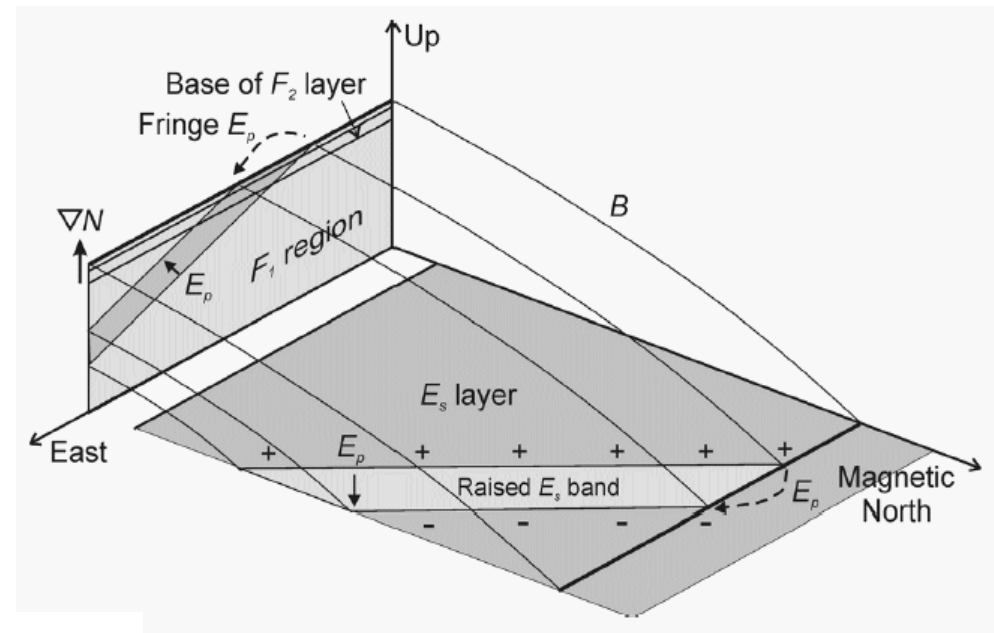




Large-Scale Wave structures (Tsunoda, GRL, 2006)



Diagram showing the development of a polarization electric field along an altitude-modulated E_s region. The E field maps to the plane over the magnetic equator that produces a displacement of the F region, a LSWS.



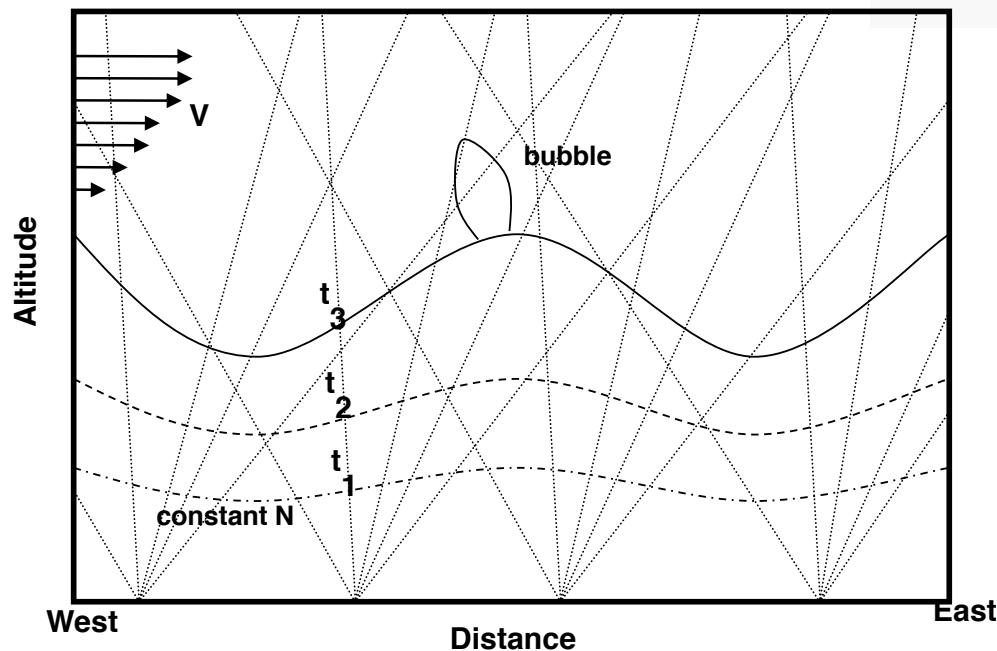
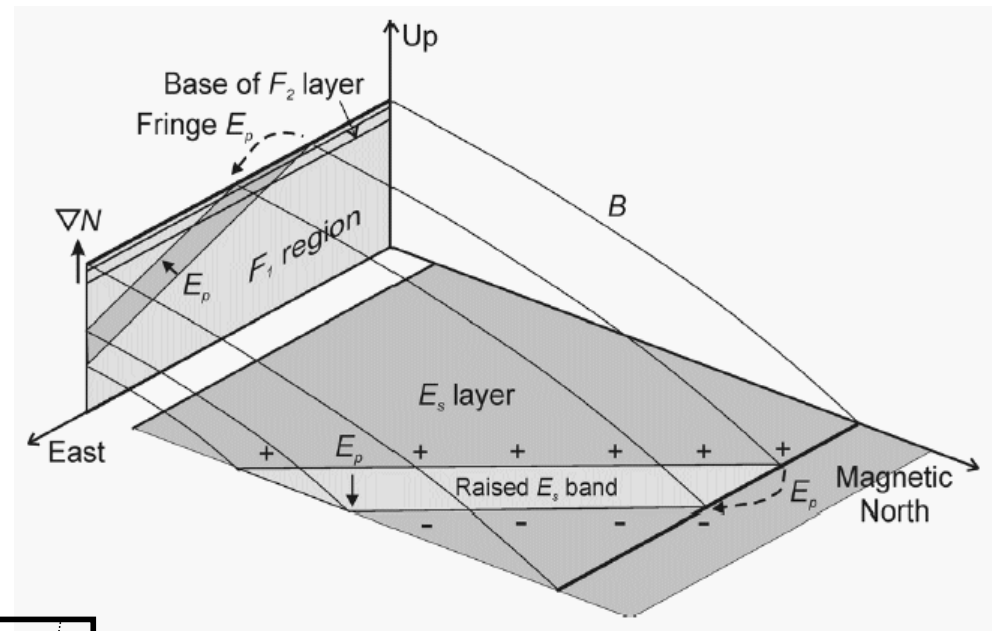
Density distributions measured during an east-to-west scan with the ALTAIR IS radar on 24 July 1979 [Tsunoda and White, 1981].



Large-Scale Wave structures (Tsunoda, GRL, 2006)



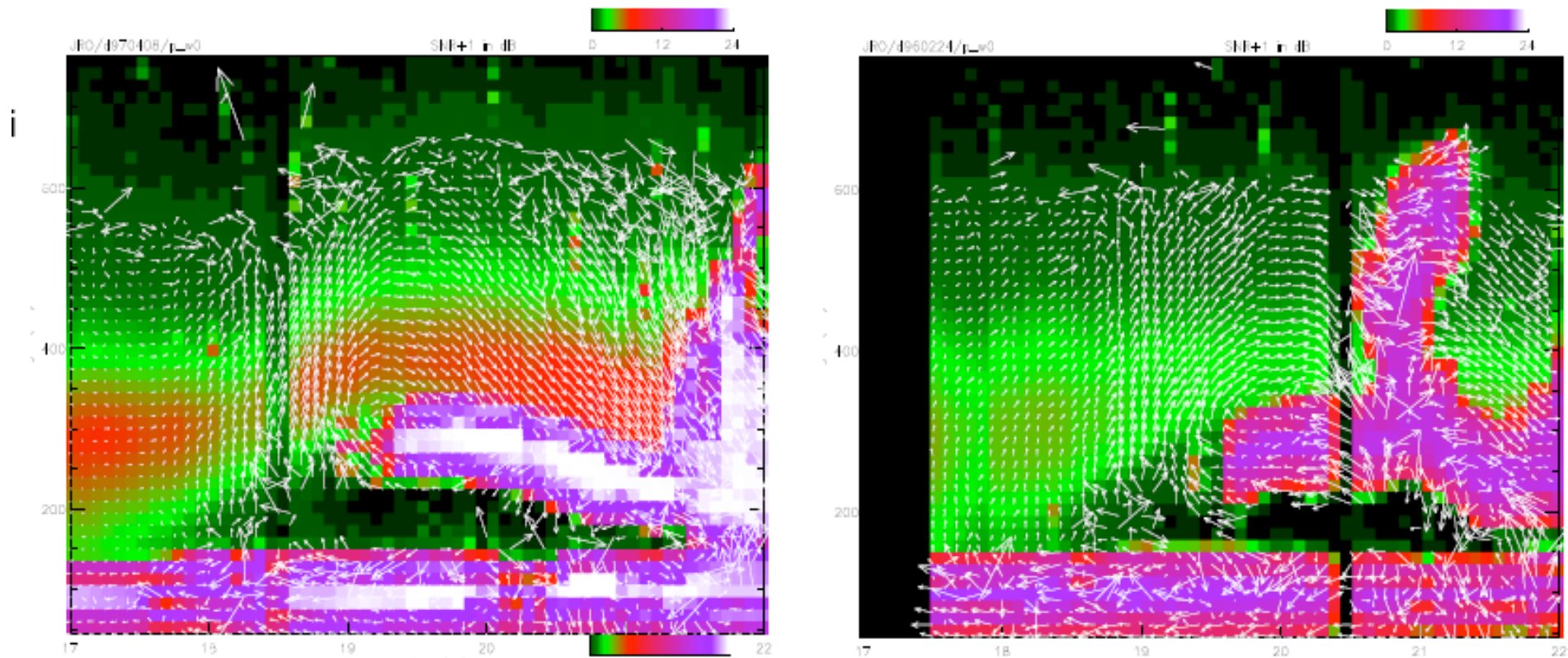
Diagram showing the development of a polarization electric field along an altitude-modulated E_s region. The E field maps to the plane over the magnetic equator that produces a displacement of the F region, a LSWS.



9 GPS receivers are presently located along the magnetic equator to observe the variability of TEC across Peru, Bolivia and the western part of Brazil.



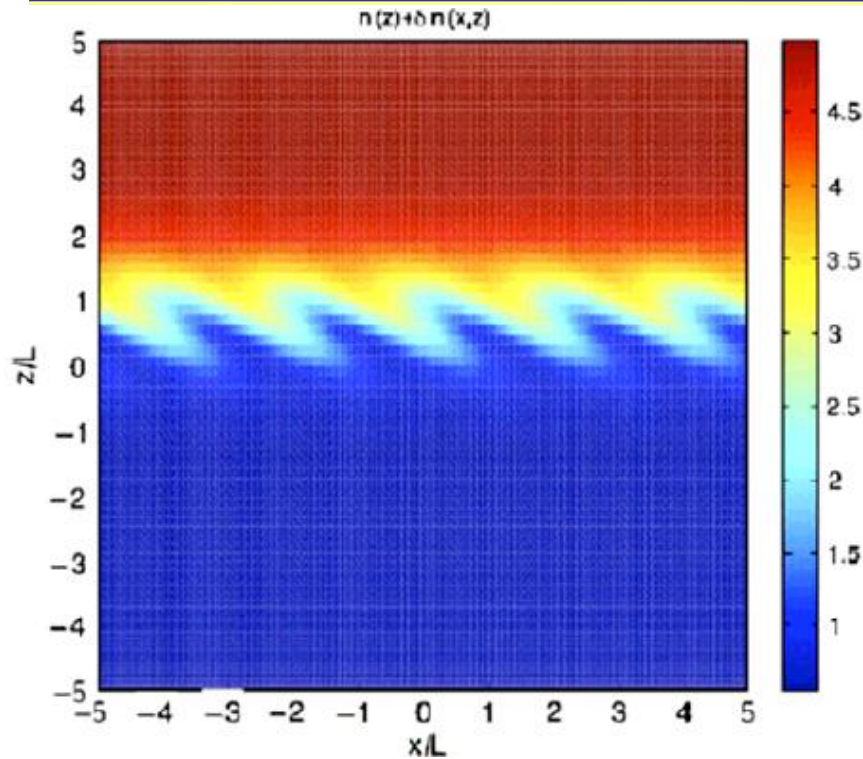
Vortex and ESF observations at JRO



Sheared zonal flows in the post-sunset equatorial F region were known since the early 80's, but the new high resolution JRO observations have shown that: (1) Equatorial Spread F develops within the sheared flow structure. (2) The shear is part of the post-sunset F-region vortex. **It is possible that vortex fragmentation seeds the initiation of ESF.**

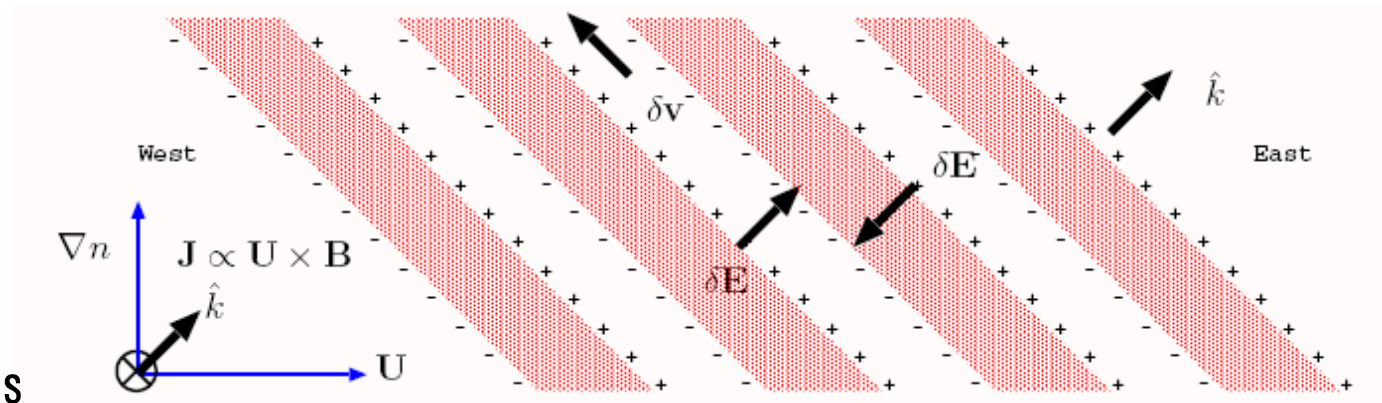


Wind driven gradient-drift Instability (Kudeki et al. 2007)



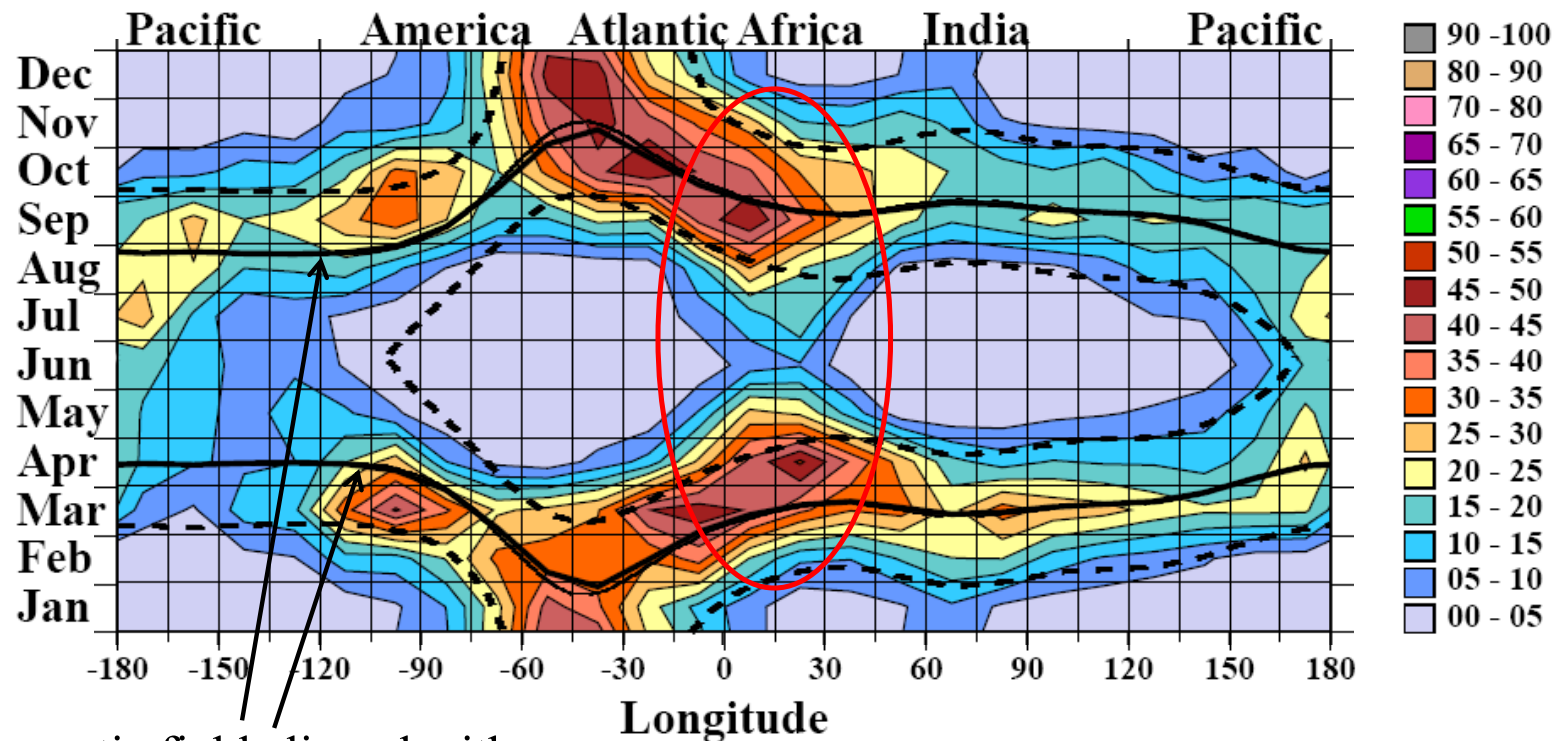
Kudeki et al. [2007] numerical simulation demonstrated that for values of the zonal wind equal to 200 m/s and gradient scale length of 20 km, the preferred scale size of the perturbation was 40 km and the growth rate equal to 200 sec, many times higher than the RT growth rate.

Sketch of the wind driven gradient drift (ExB) instability. The eastward wind drives an upward Pedersen current that polarizes the density perturbations that have westward tilted wave-fronts.





DMSP EPB Rates 1999 - 2002



Magnetic field aligned with terminator (Tsunoda 1985)

L. C. Gentile et al. 2006: A global climatology for equatorial plasma bubbles

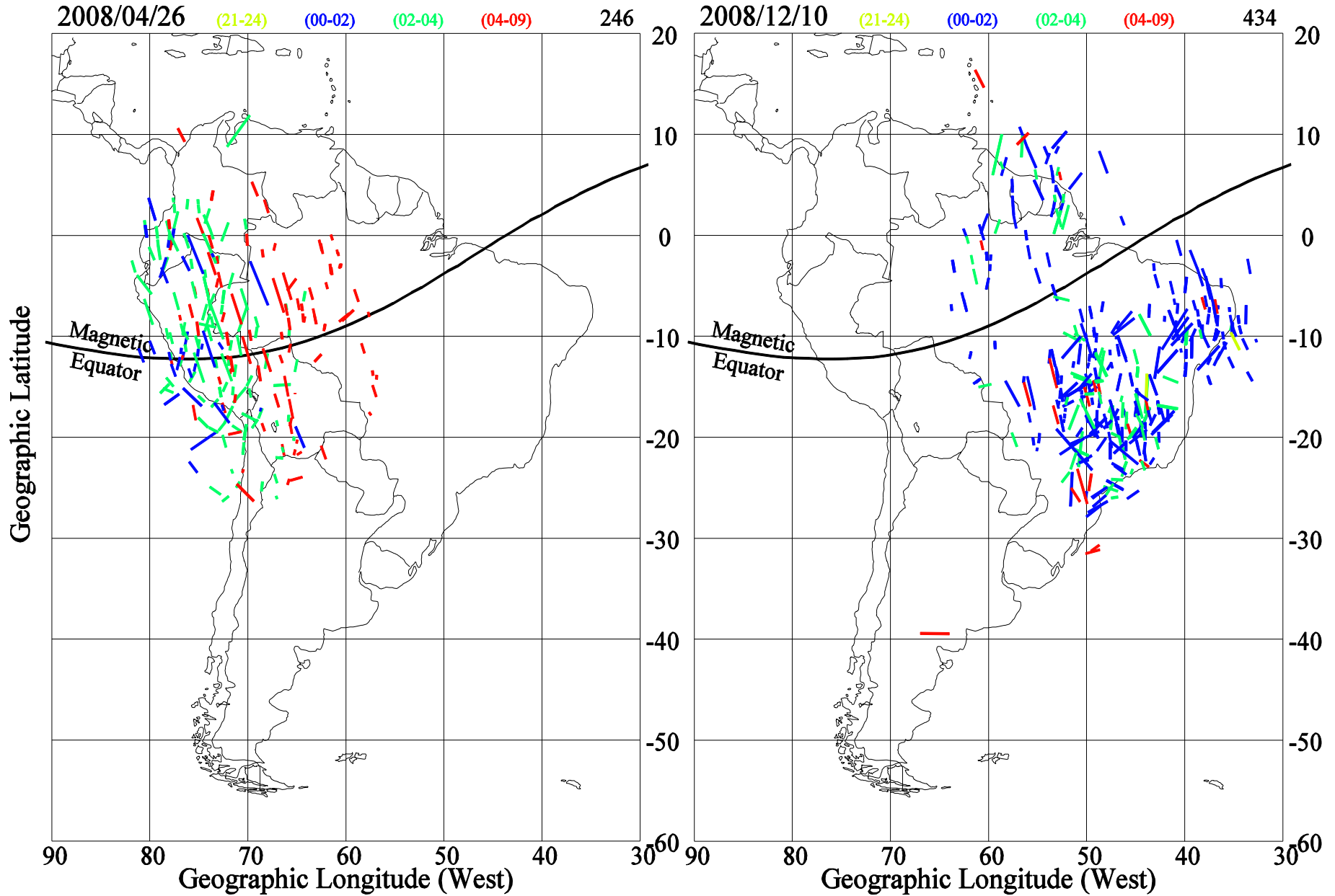
Within the African sector:

- EPBs occur throughout the year
- Seasonal occurrence moves toward summer solstice with increasing longitude
- The occurrence rate decreases with increasing longitude

Question: do GPS EPBs/scintillation observations in Africa share these characteristics?

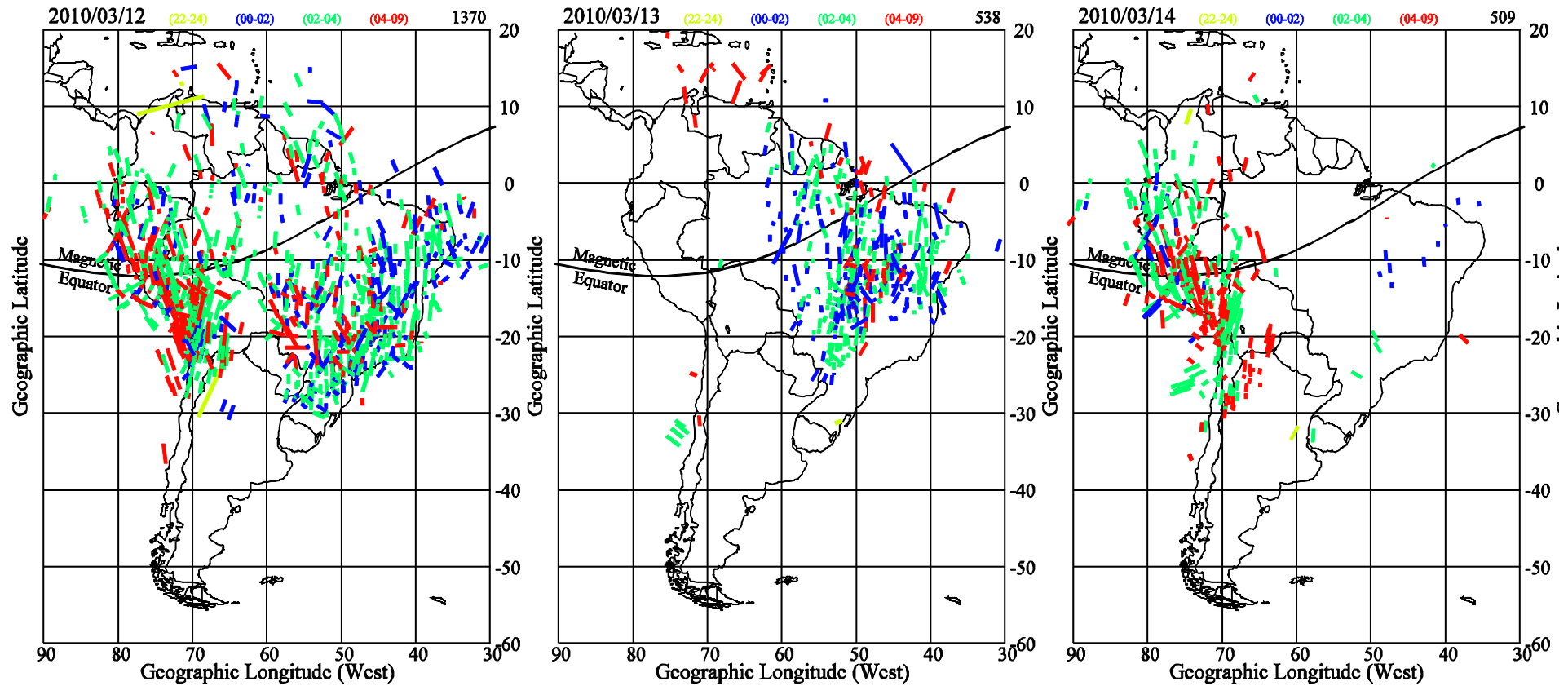


Seasonal Variability of TEC depletions that follow Tsunoda's 1985





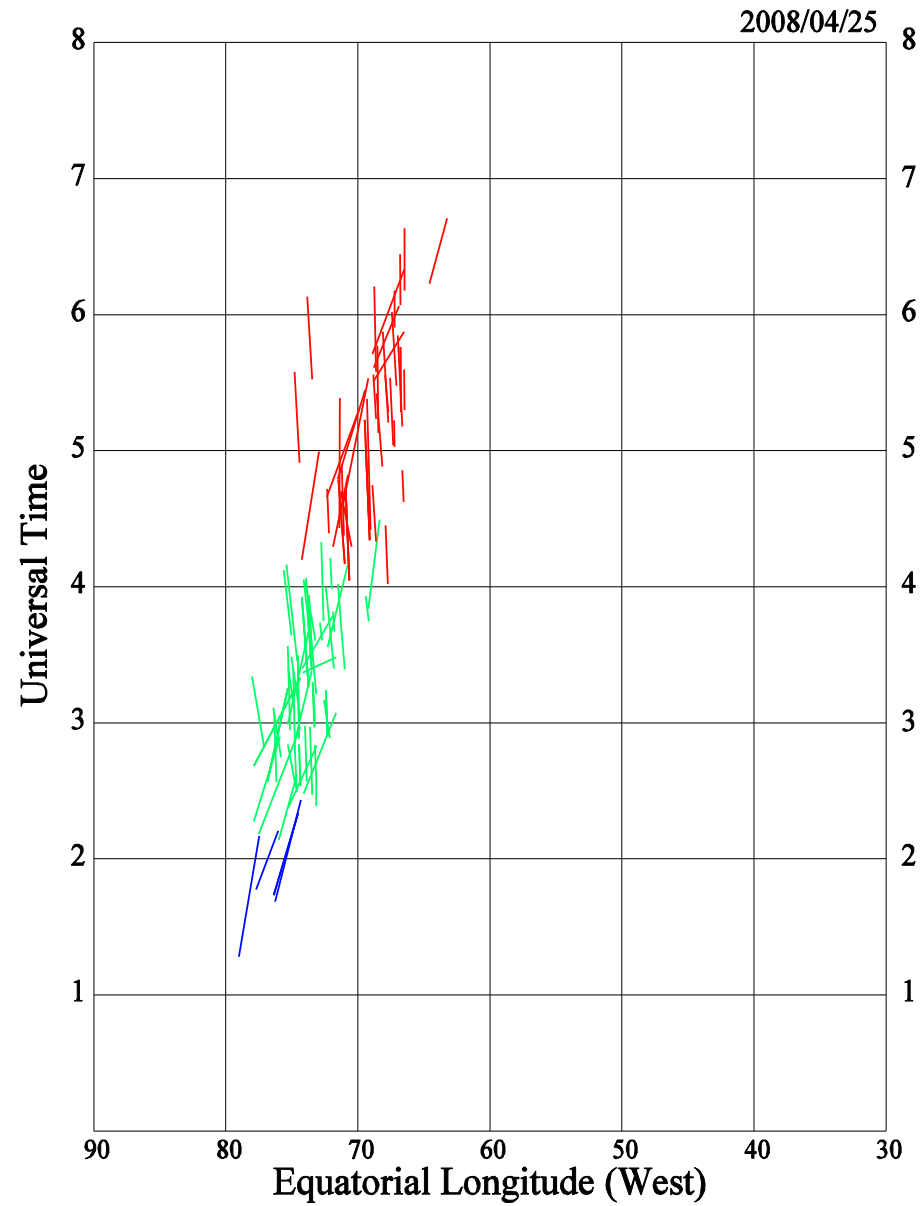
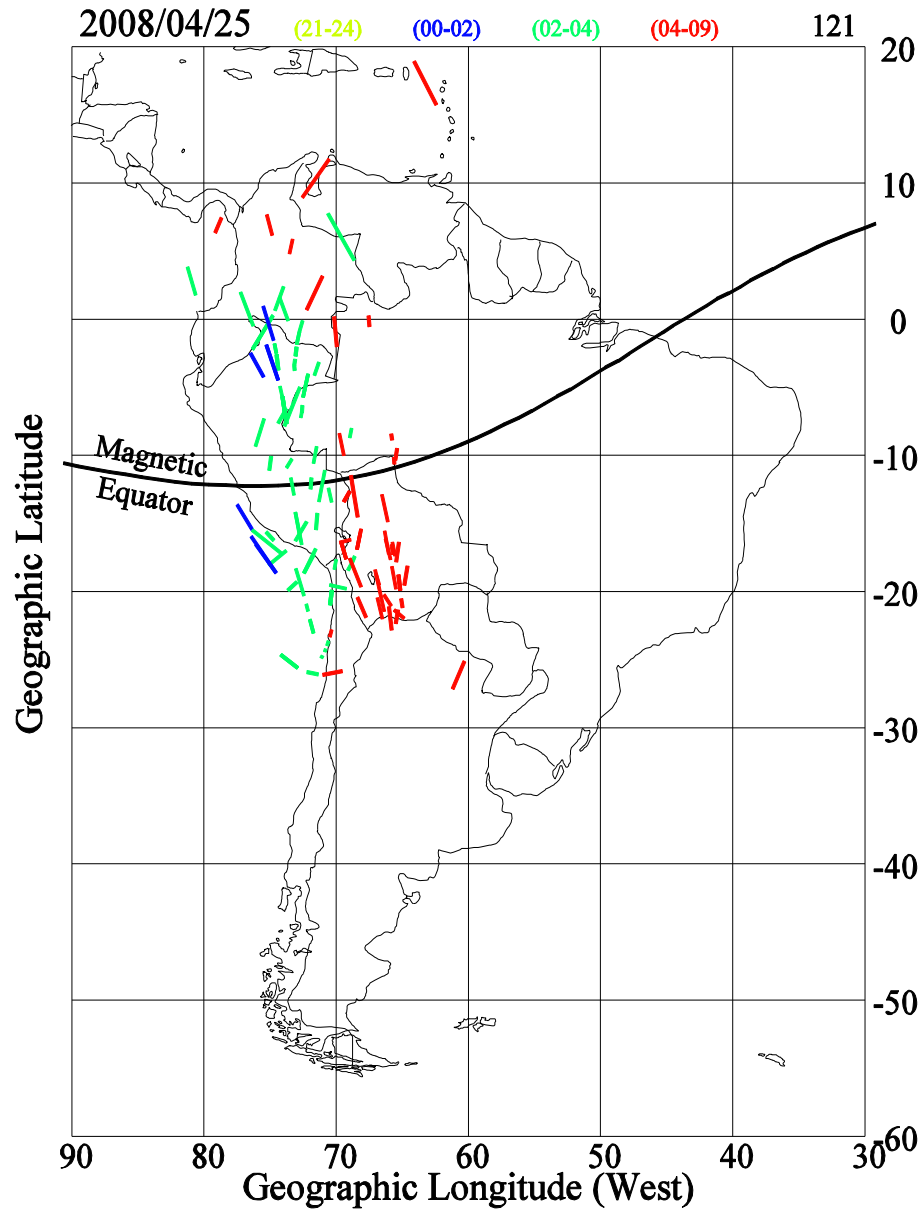
TEC depletions observed on 3 consecutive days (March 12, 13, 14, 2010)





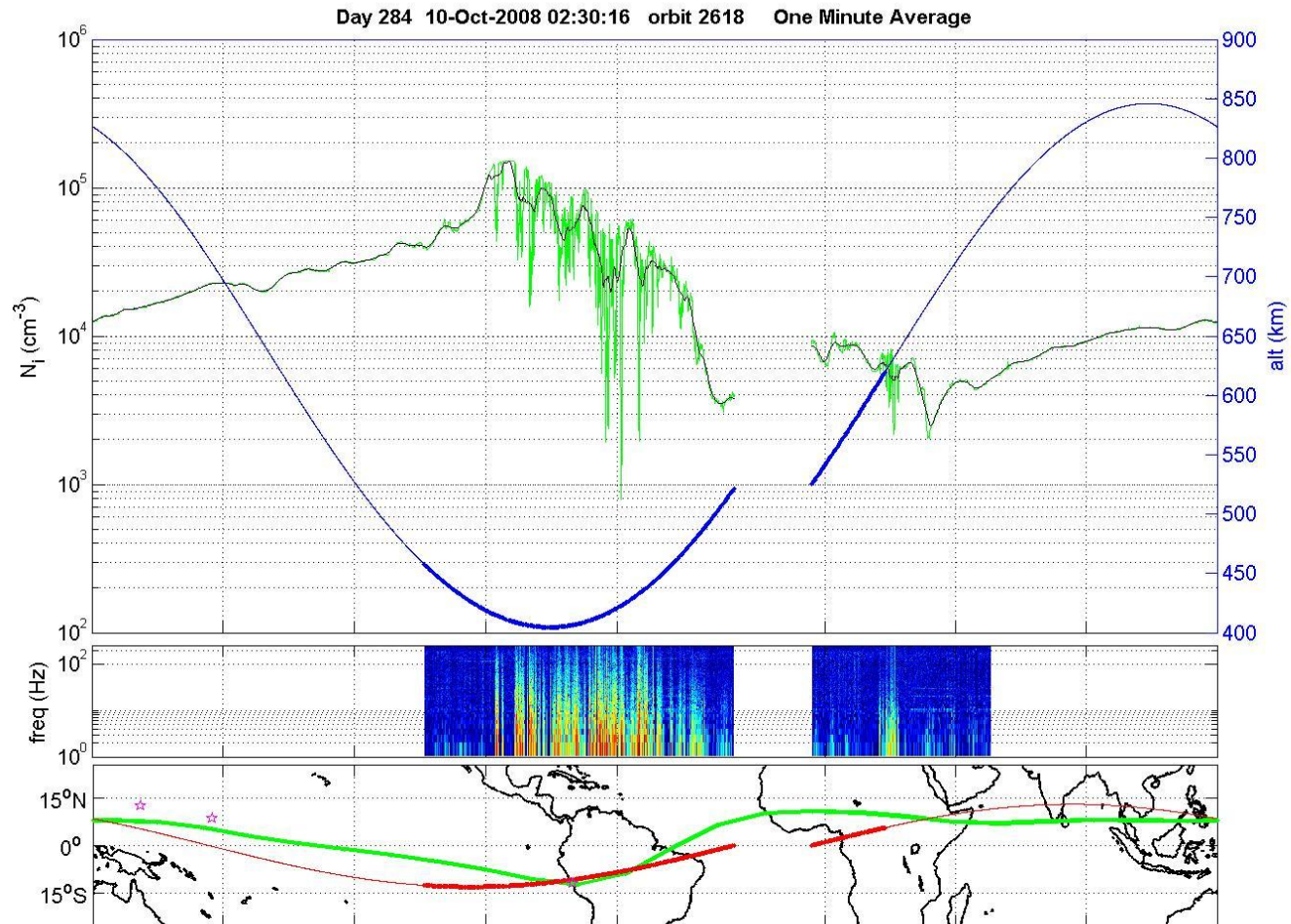
TEC depletions observed on April 25, 2008

Same TEC depletions mapped to Eq. vs UT





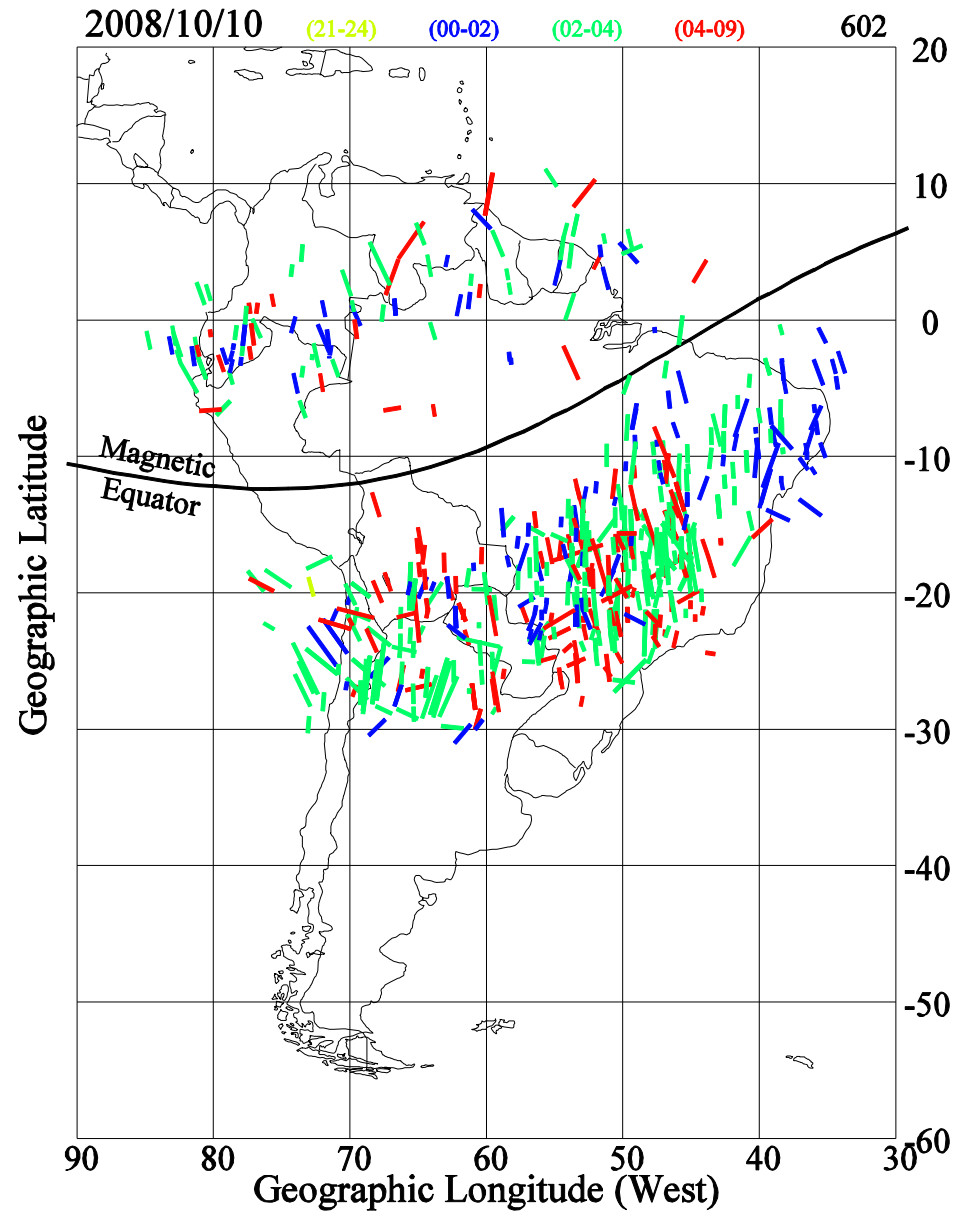
Extreme Spread F conditions (Oct 10, 2008)



GLON	171.3	213.2	255.4	297.5	003.9	045.8	087.7	129.5
GLAT	-01.2	-10.1	-13.0	-08.5	+01.1	+10.1	+13.0	+08.5
GALT	697	527	419	421	541	712	831	826
MLON	242.7	285.4	327.3	008.4	075.0	117.2	159.1	200.0
MLAT	-05.5	-08.0	-05.7	+04.8	-11.9	+01.1	+04.4	+00.5
UT	03:21	03:34	03:45	03:56	02:31	02:43	02:56	03:08
LT	15:00	18:00	21:00	00:00	03:00	06:00	09:00	12:00

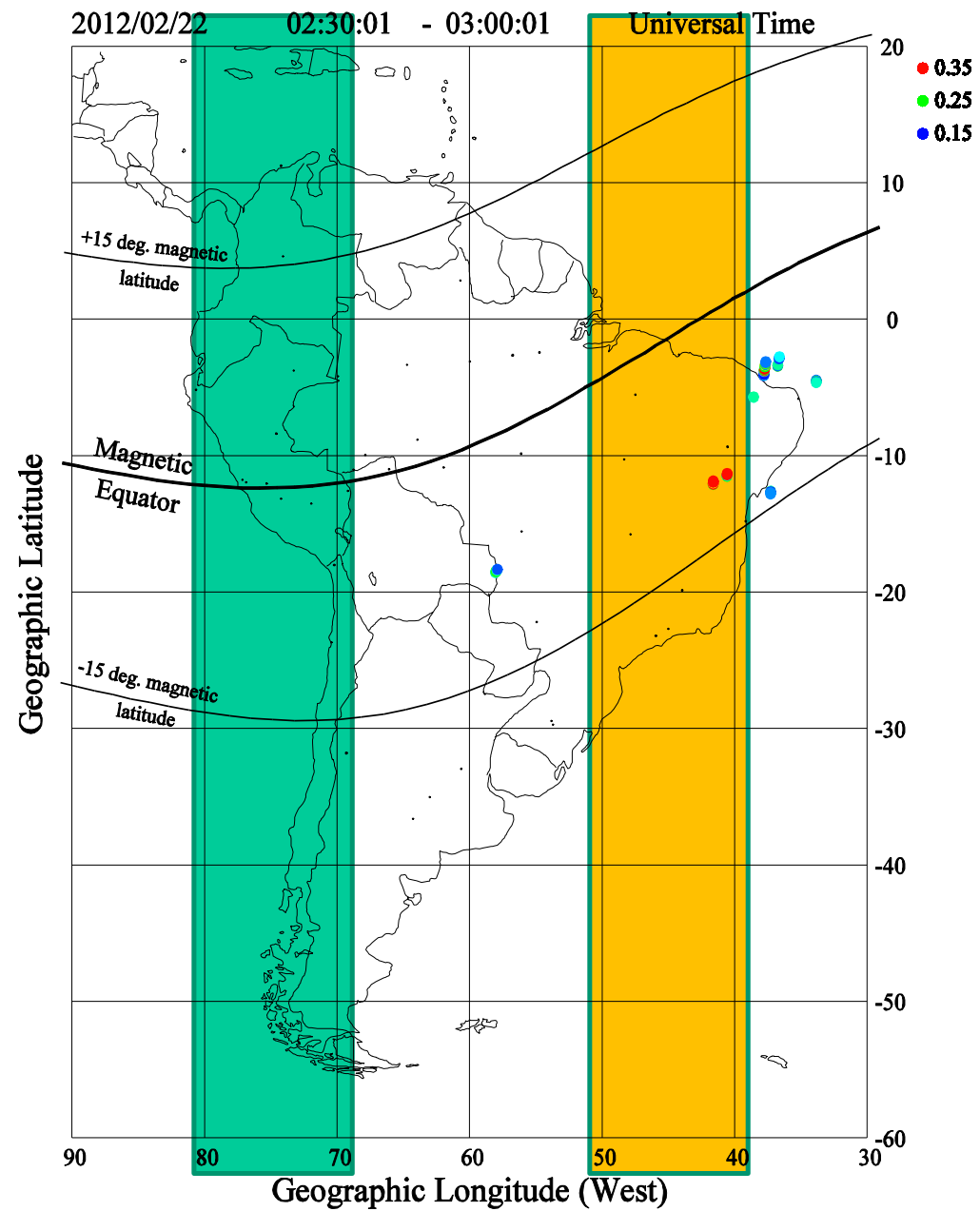


TEC depletions observed on Oct 10, 2008



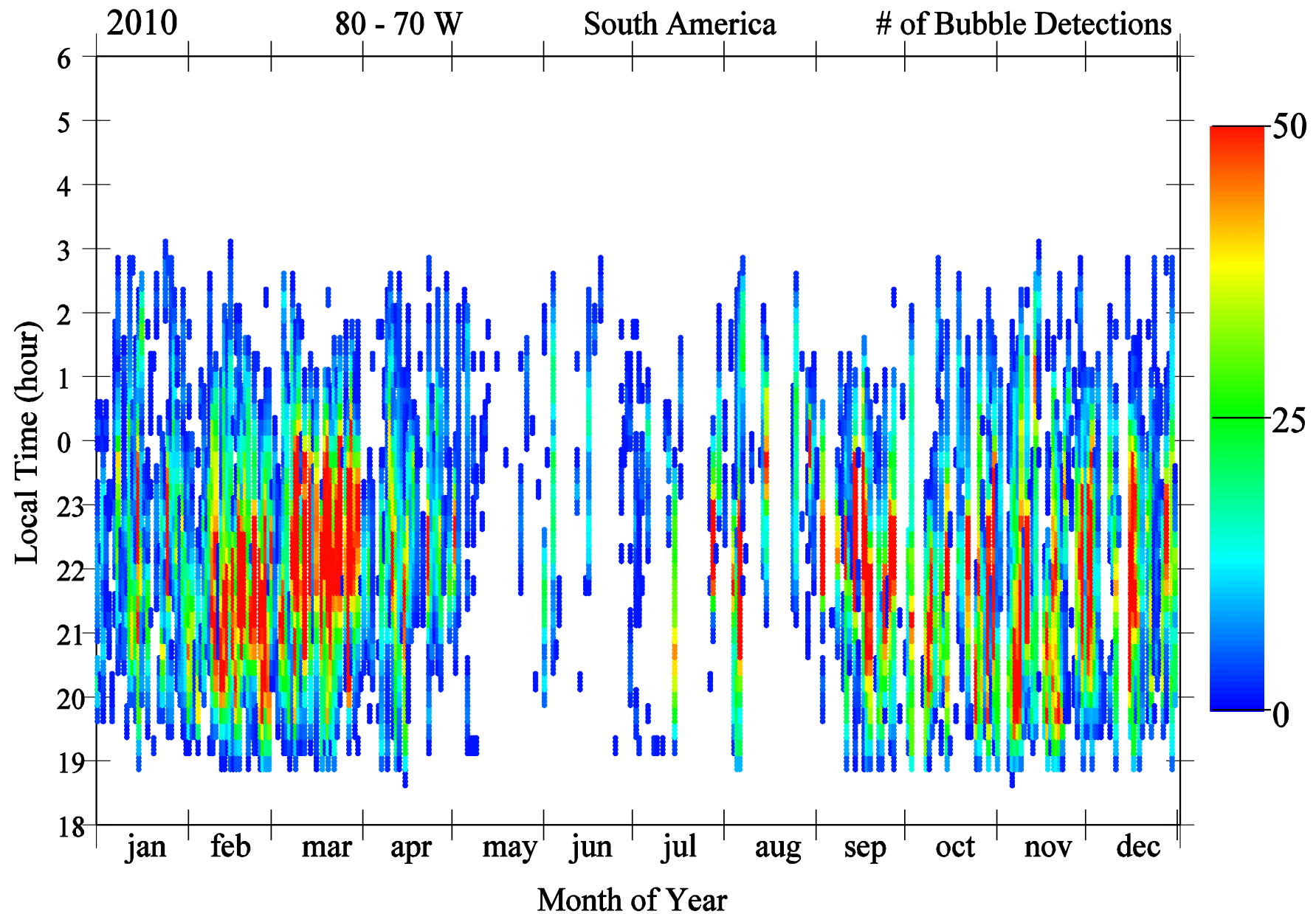


TEC depletions and TIDs in Two different sectors



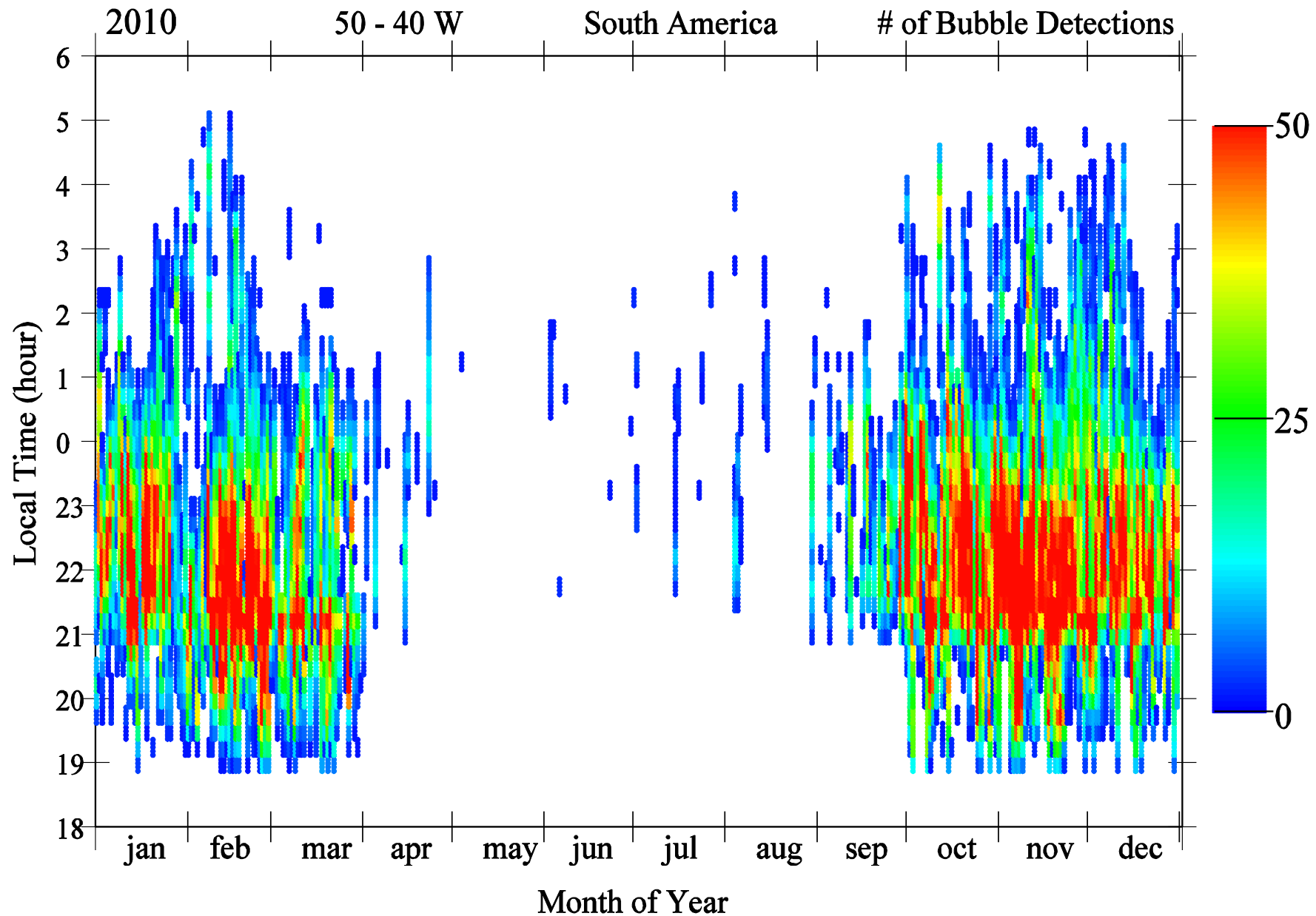


Number of TEC depletion detections as a function of Local time and day of Year between 80 and 70 W



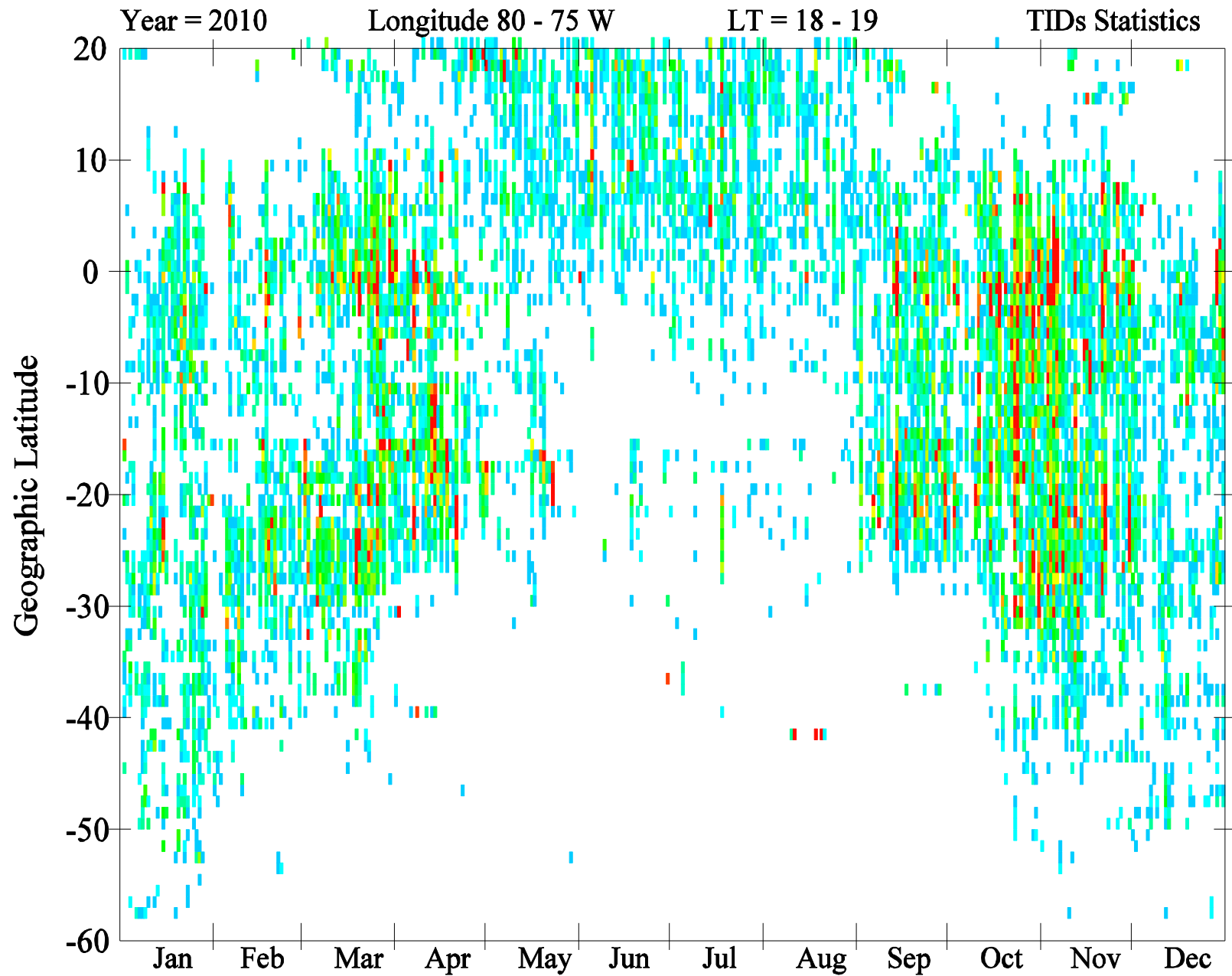


Number of TEC depletion detections as a function of Local time and day of Year between 50 and 40 W



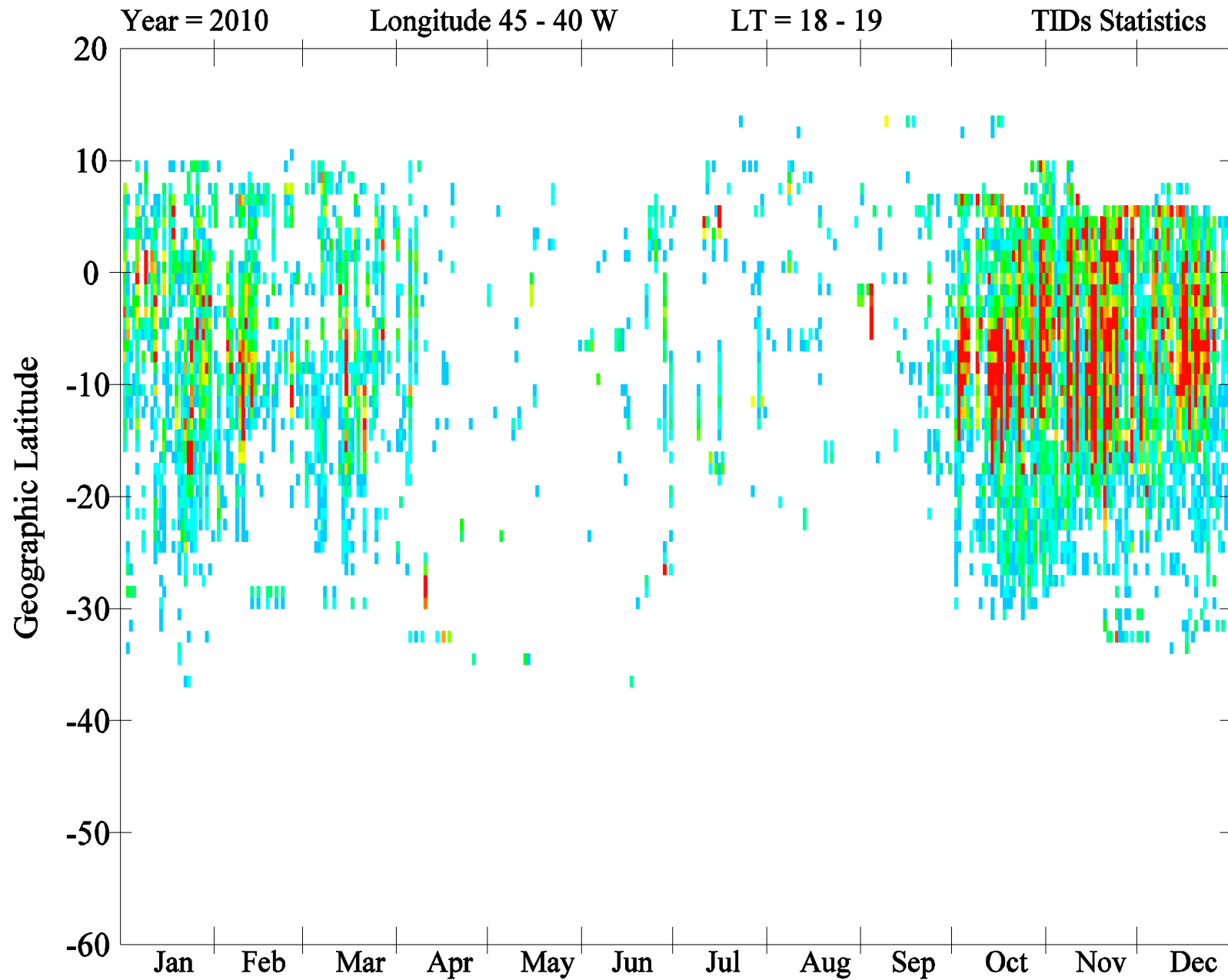


TID Statistics between 80 and 75 W vs. Latitude and day of year



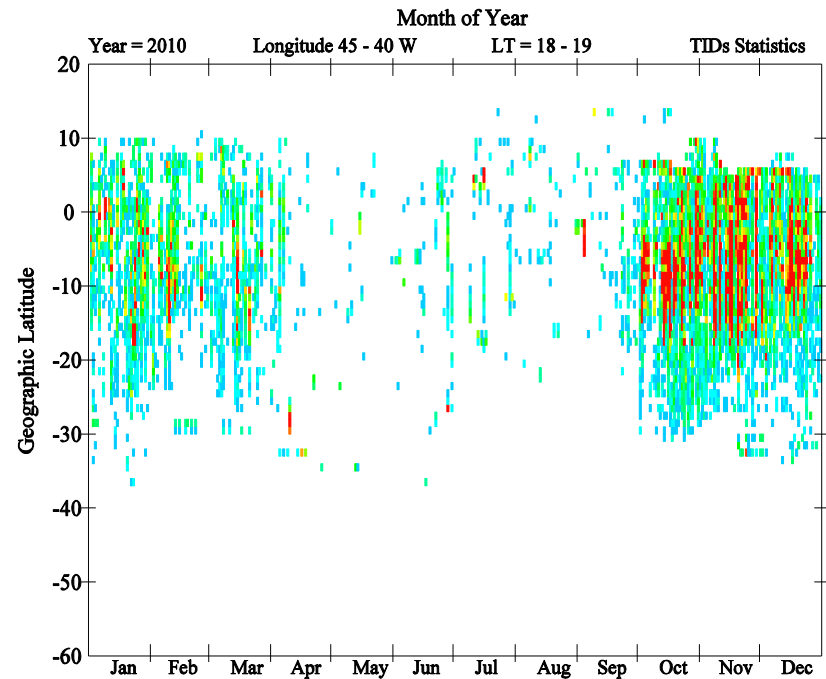
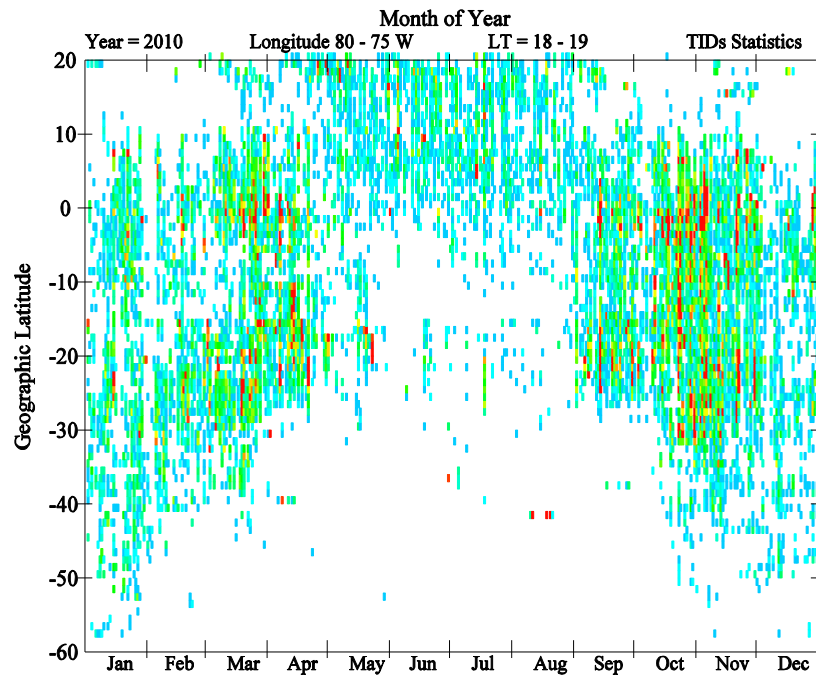
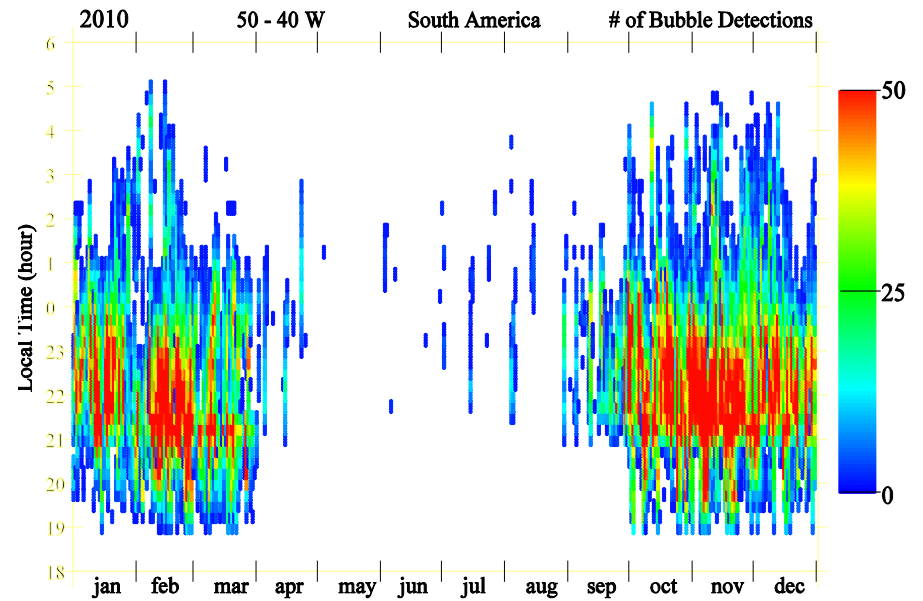
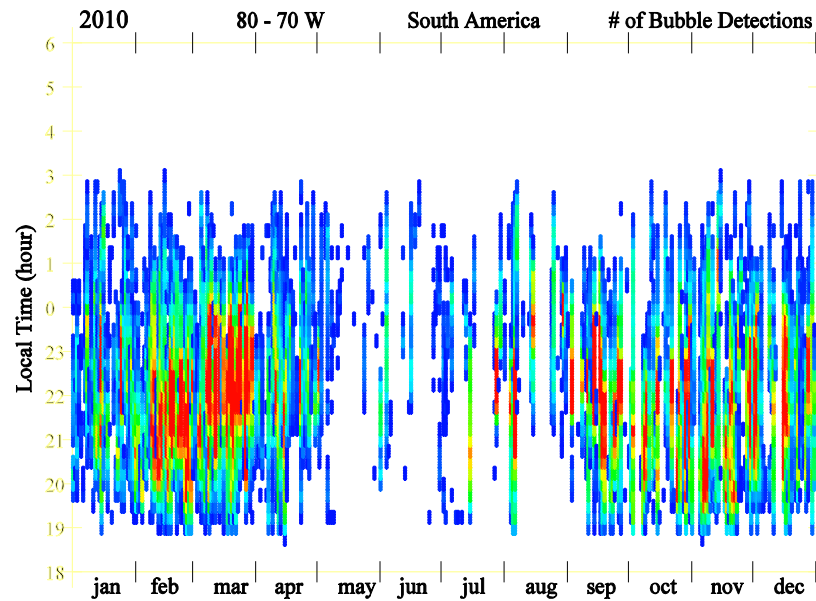


TID Statistics between 80 and 75 W vs. Latitude and day of year



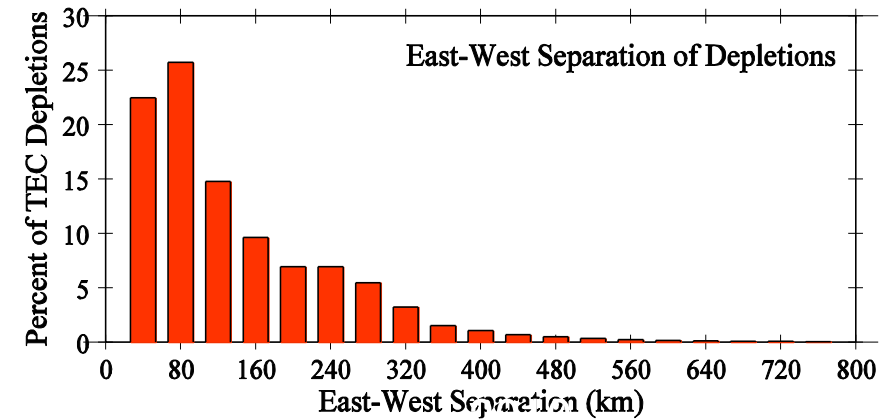
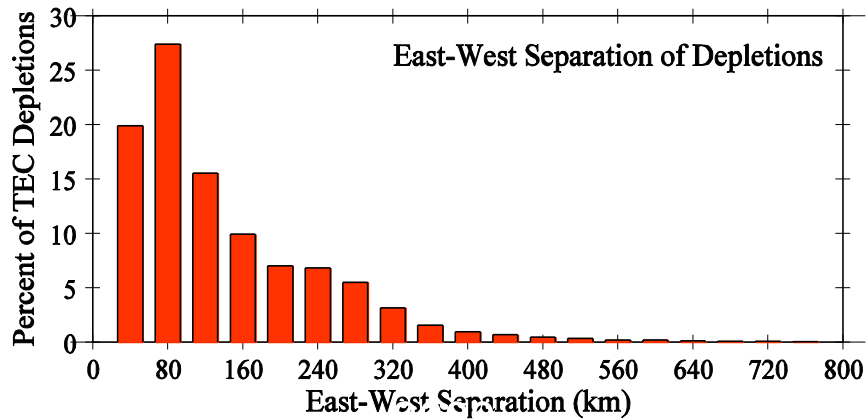
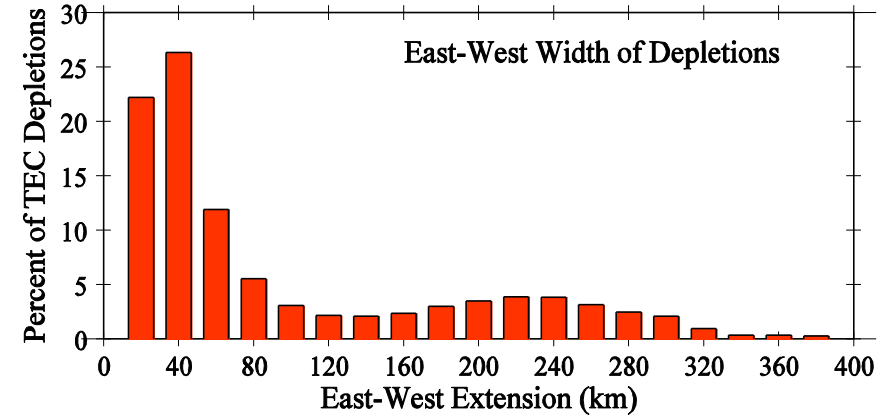
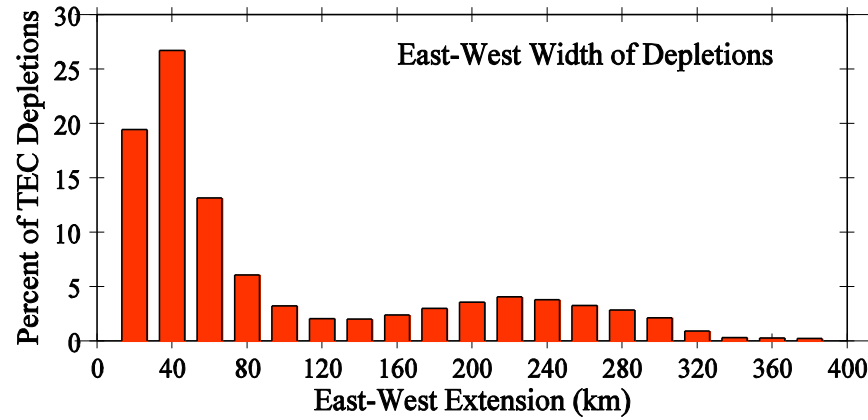


Comparison of TEC depletion statistics and TIDs over South America





Statistics of the width and separation of TEC depletions measured in South America

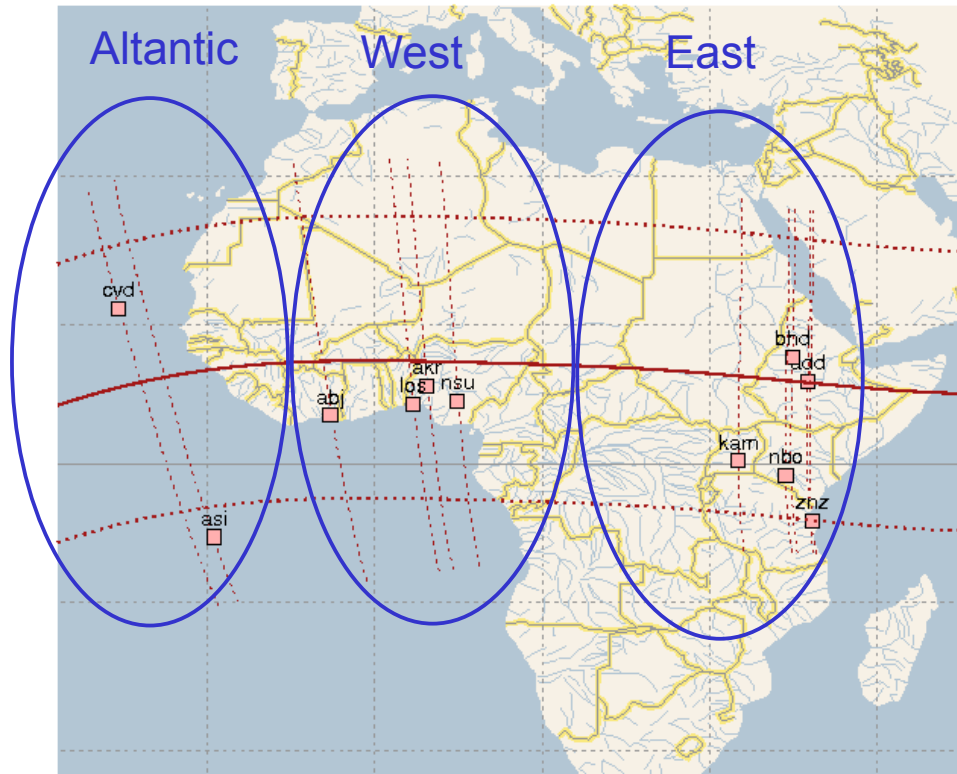


2009

2010



SCINDA Ground Stations in Africa (2010)



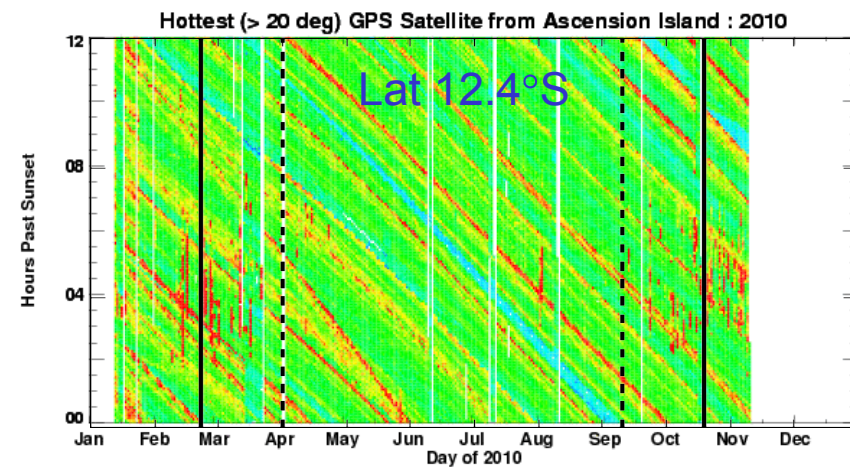
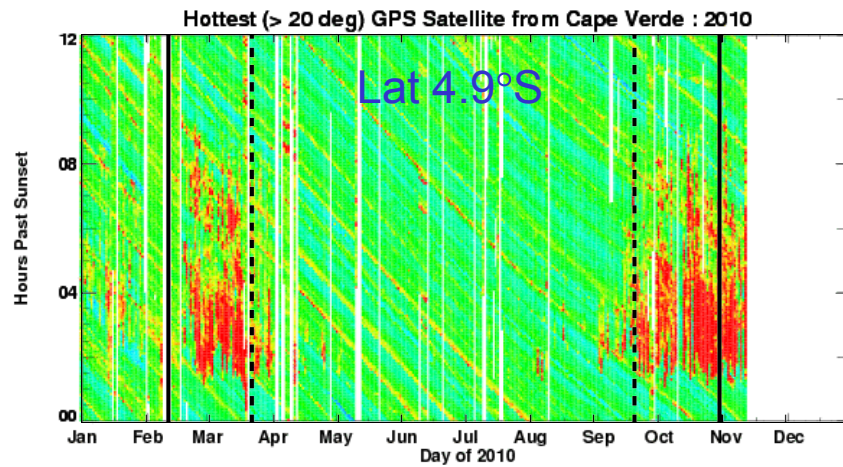
Station	Location
Abidjan, Ivory Coast	5.3°N, 4.0°W, dip 3.5°S
Addis Ababa, Ethiopia	9.0°N, 38.8°E, dip 0.1°N
Ascension Island	7.9°S, 14.4°W, dip 12.4°S
Bahir Dar, Ethiopia	11.5°N, 37.4°E, dip 2.5°N
Sal, Cape Verde	16.6°N, 22.9°W, dip 4.9°N
Ilorin, Nigeria	8.4°N, 4.7°E, dip 1.9°S
Kampala, Uganda	0.3°N, 32.6°E, dip 9.2°S
Lagos, Nigeria	6.5°N, 3.4°E, dip 3.1°S
Nairobi, Kenya (west)	1.3°S, 36.8°E, dip 10.7°S
Nairobi, Kenya (east)	1.1°S, 37.0°E, dip 10.5°S
Nsukka, Nigeria	6.8°N, 7.4°E, dip 3.0°S
Zanzibar, Tanzania	6.2°S, 39.2°E, dip 15.9°S



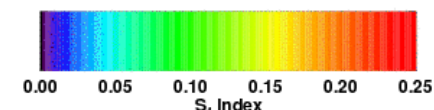
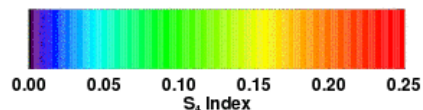
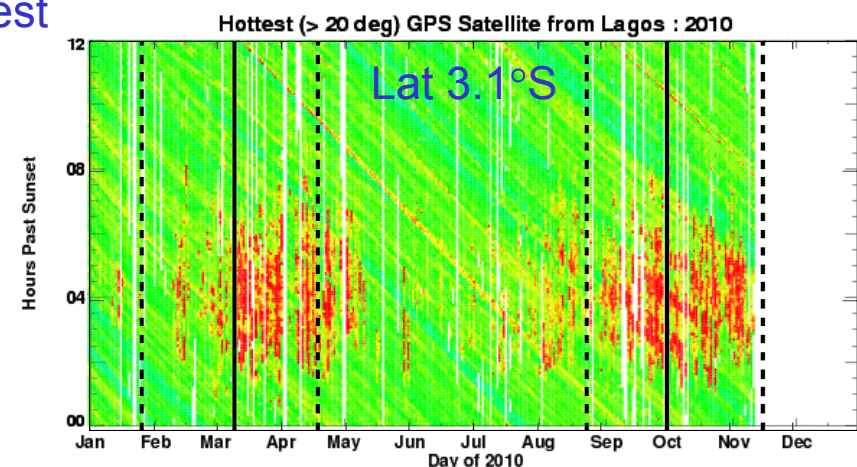
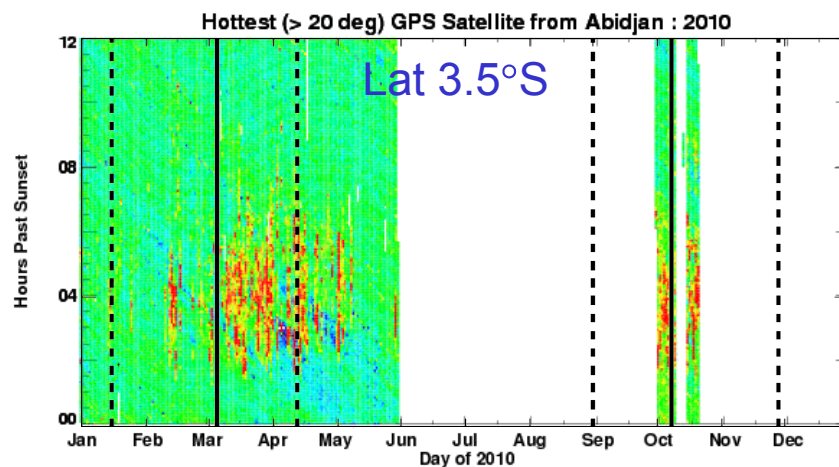
Atlantic and West Africa Comparison



Atlantic



West



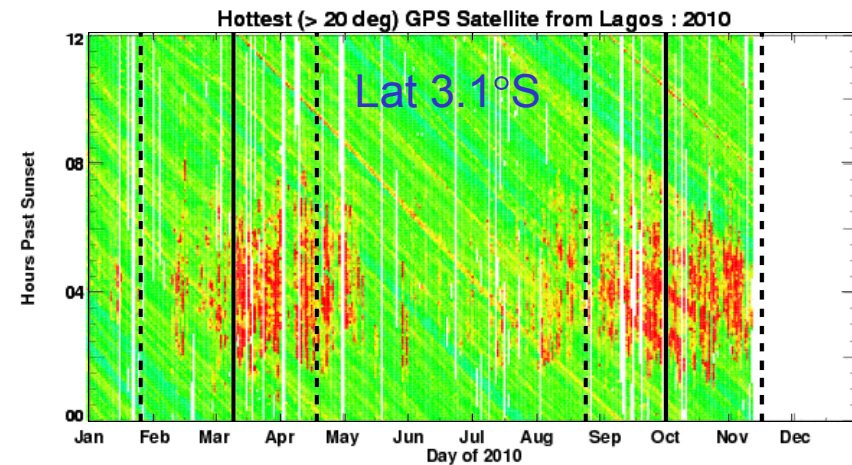
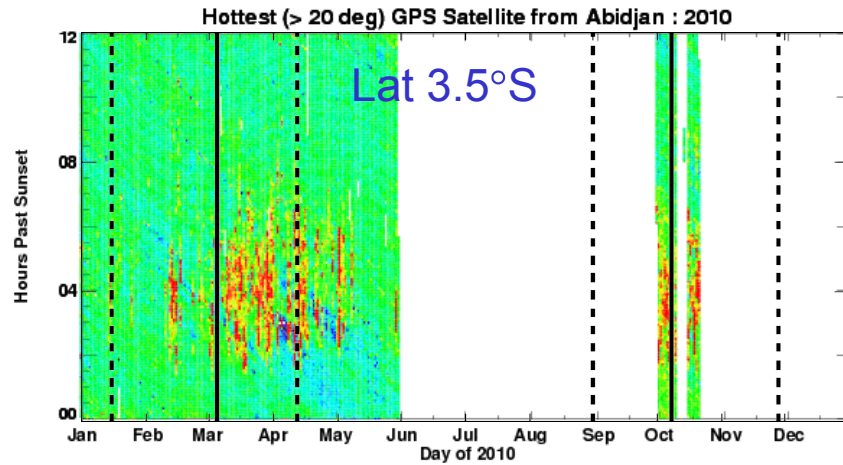
Atlantic (e.g. CV) has most intense, longest lasting, and highest occurrence rate in-season. Bubbles typically don't rise high enough to reach dip latitude of Ascension during solar minimum.



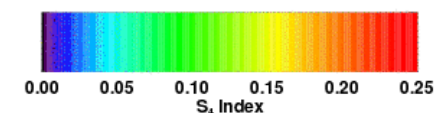
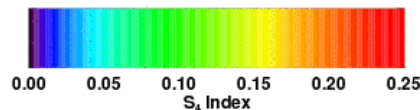
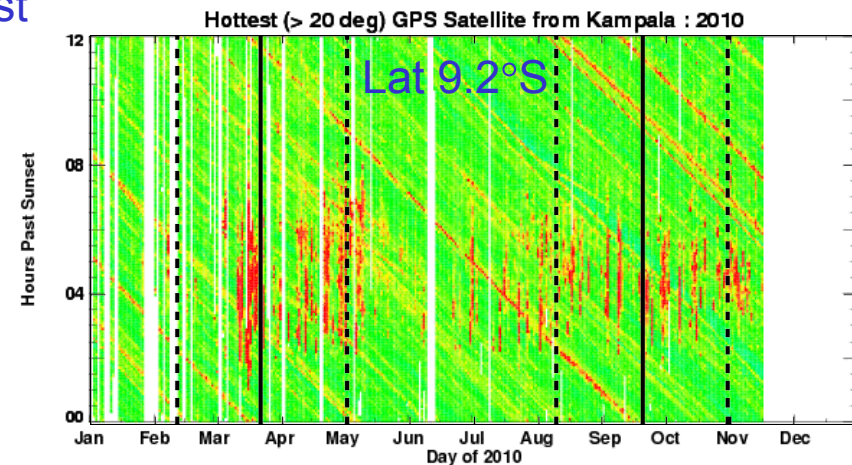
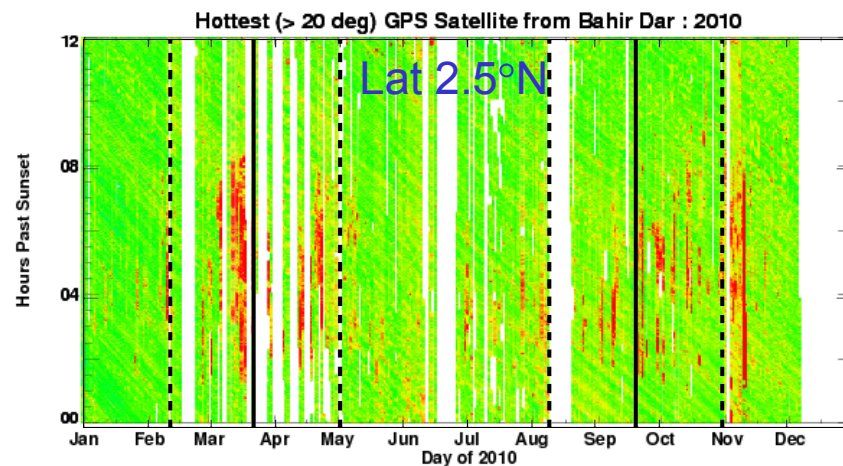
East and West Africa Comparison



West



East



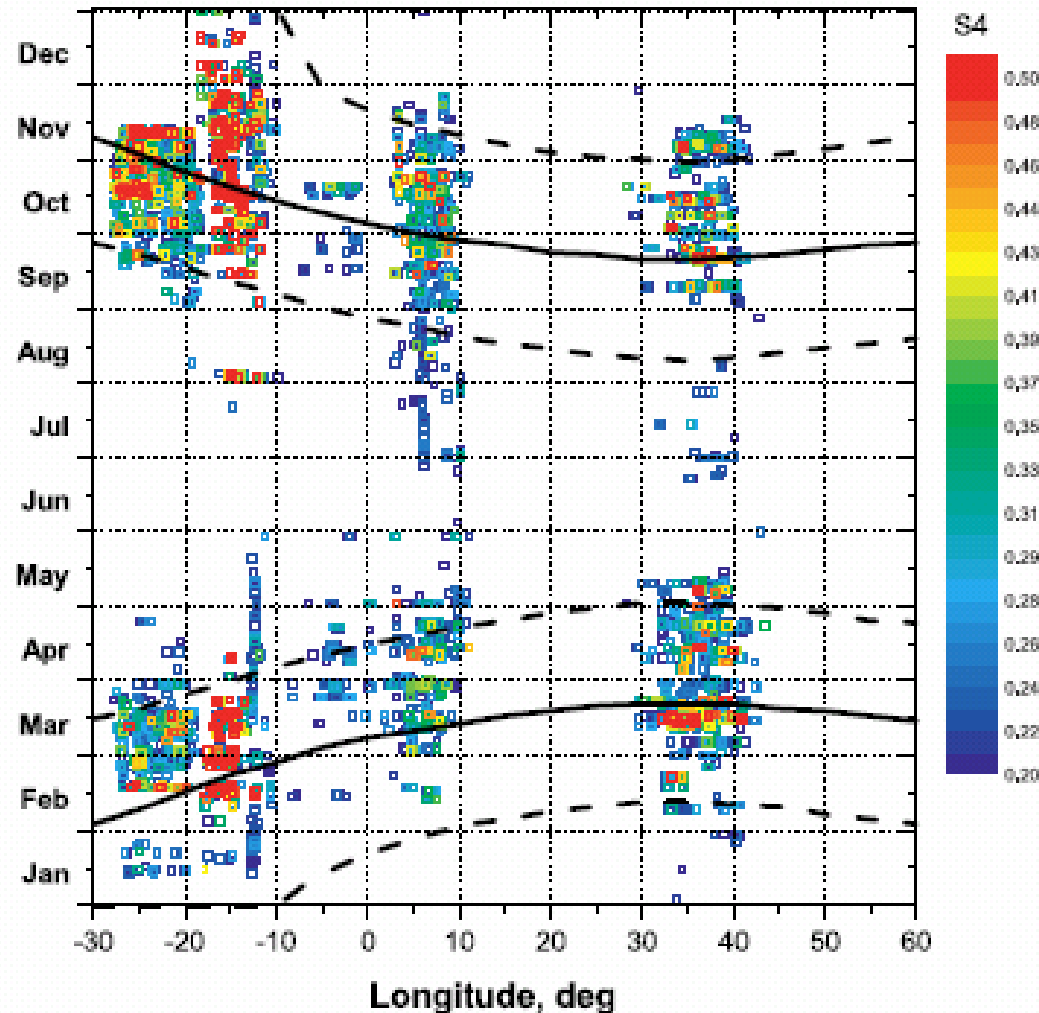
Seasonal occurrence shifts toward summer solstice when moving from west to east.
Fewer occurrences in season, shorter duration.



Distribution of GPS scintillations intensity



2010



The most intense GPS scintillations are observed when solar terminator is aligned with the geomagnetic field lines. This conditions is best satisfied during equinoxes.



Bubble Detection Algorithm (Seemala and Valladares)



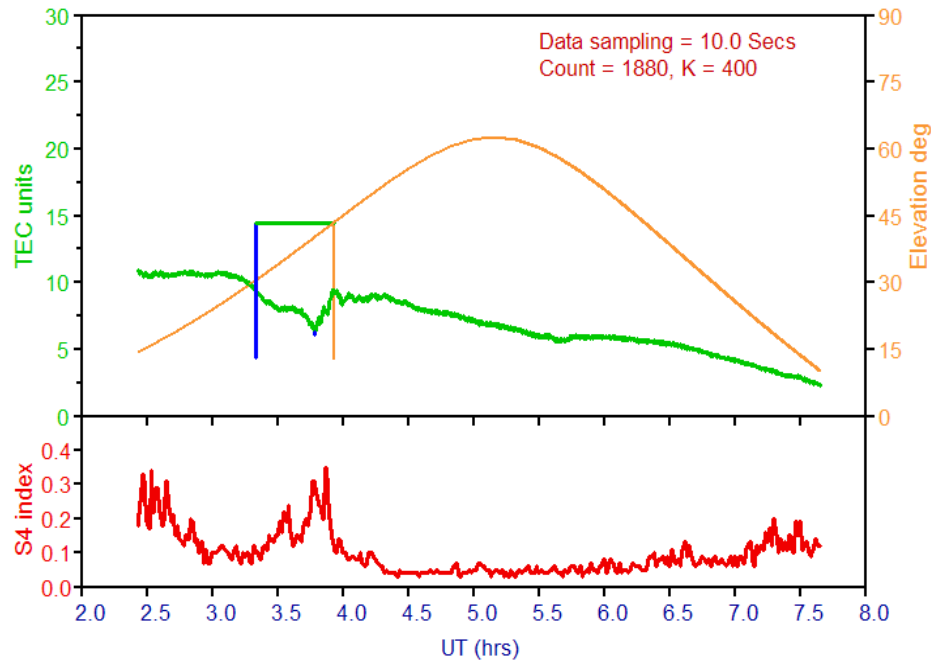
- The depletions are detected using an automated technique which is applied to the TEC trace for each GPS satellite pass and from each ground station in Africa.
- Depletions are identified by bandpass filtering the vertical TEC from each GPS satellite, and testing the result for variations of few TEC units below and above zero.
- In order to detect both narrow and wide TEC depletions, we use two spectral bands that select depletion structures lasting 3 – 40 min and also 25 - 120 min.
- The bubble detection is confirmed if the elevation angle is above 30° and the TEC recovers to a value close to the starting TEC.
- False detections arising due to TEC gradients at low elevation angles and data breaks are eliminated.



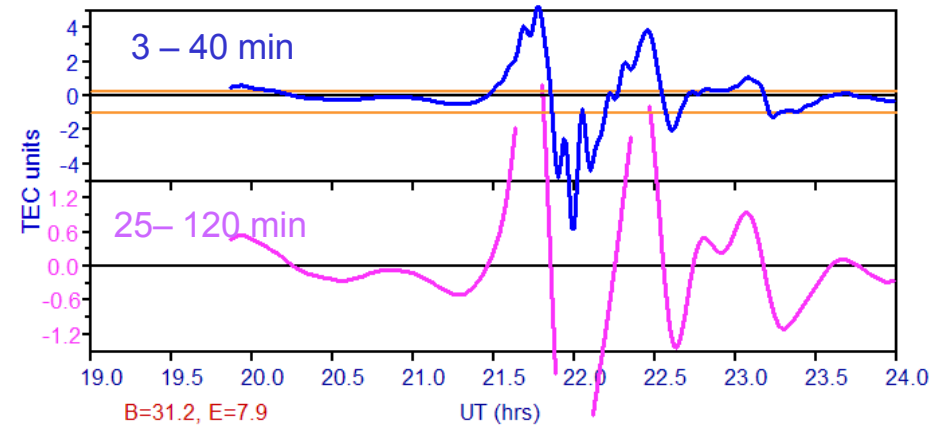
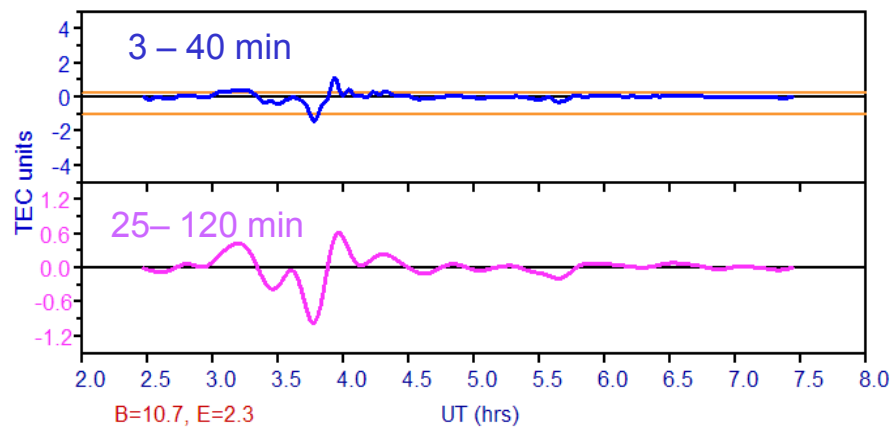
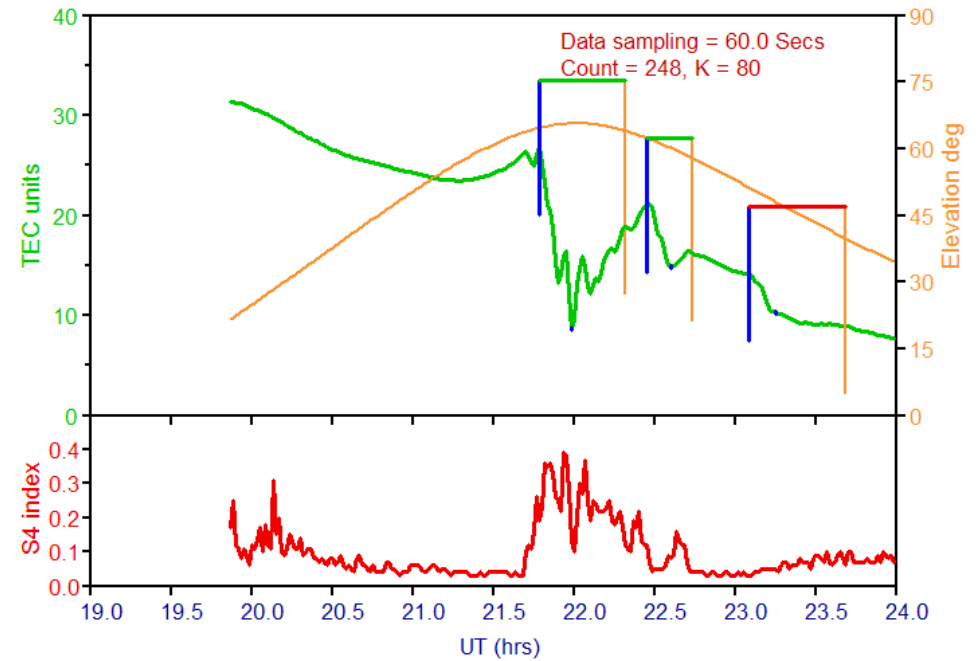
Bubble Detection Algorithm (continued)



13 Feb 2008, PRN14, Alta Floresta, Brazil

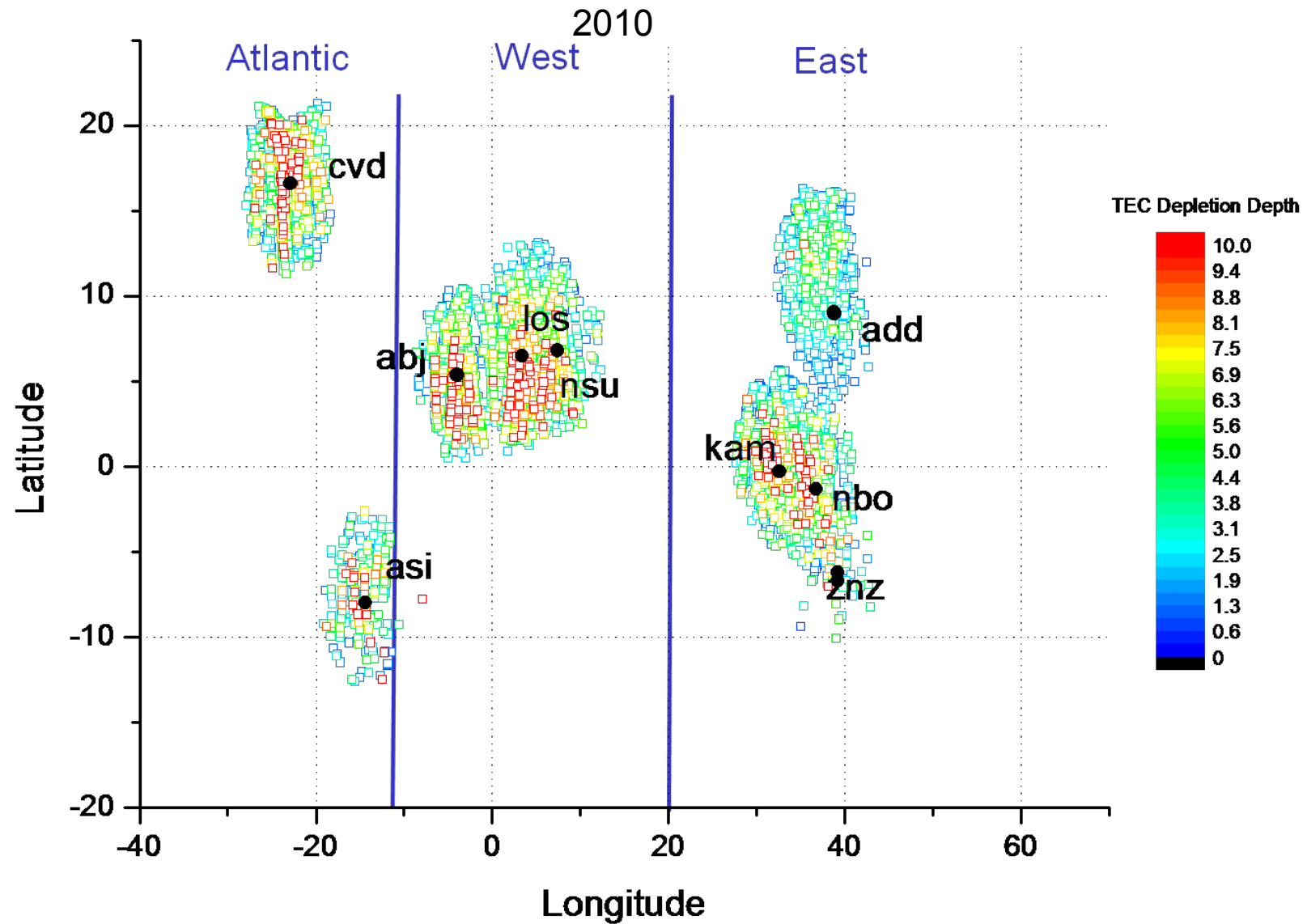


21 Oct 2010, PRN17, Ascension Island





SCINDA EPB coverage map

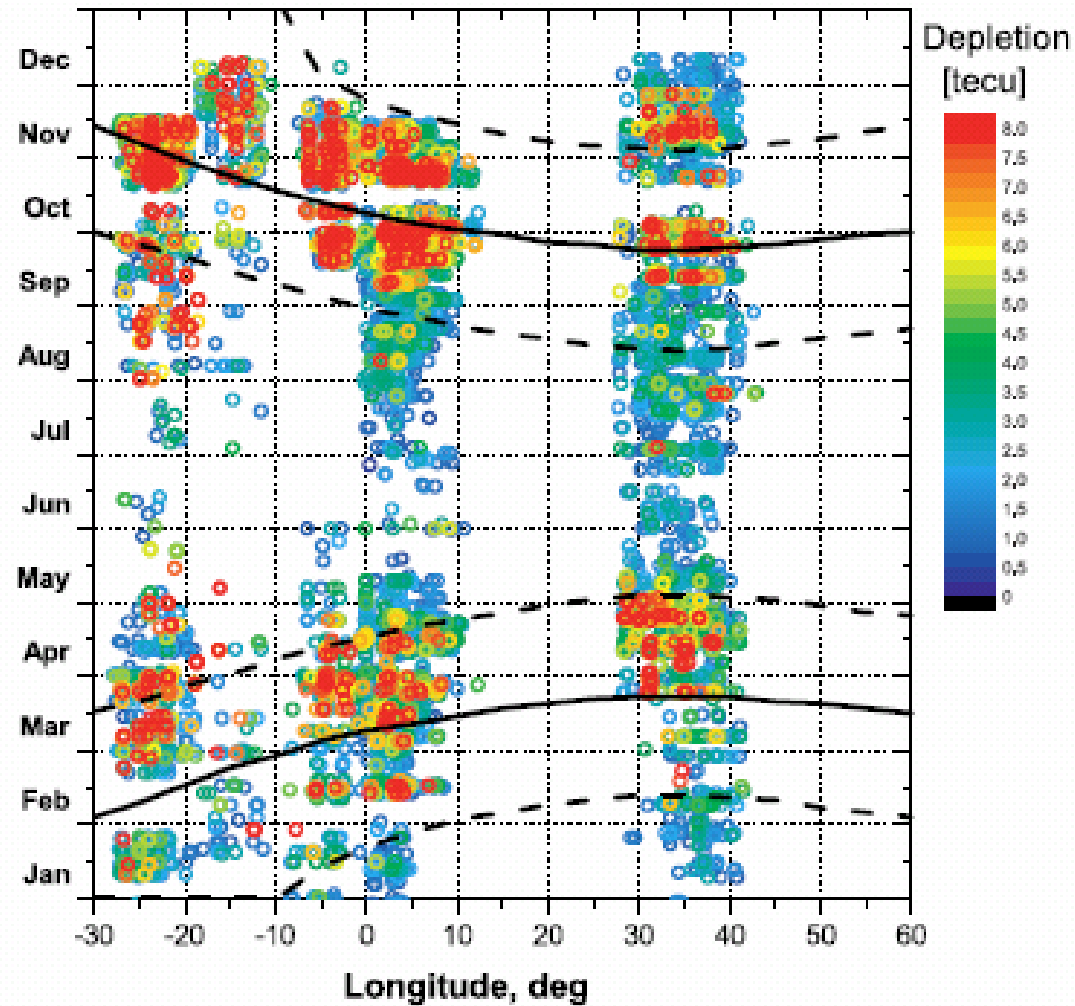




Climatology of EPBs intensity



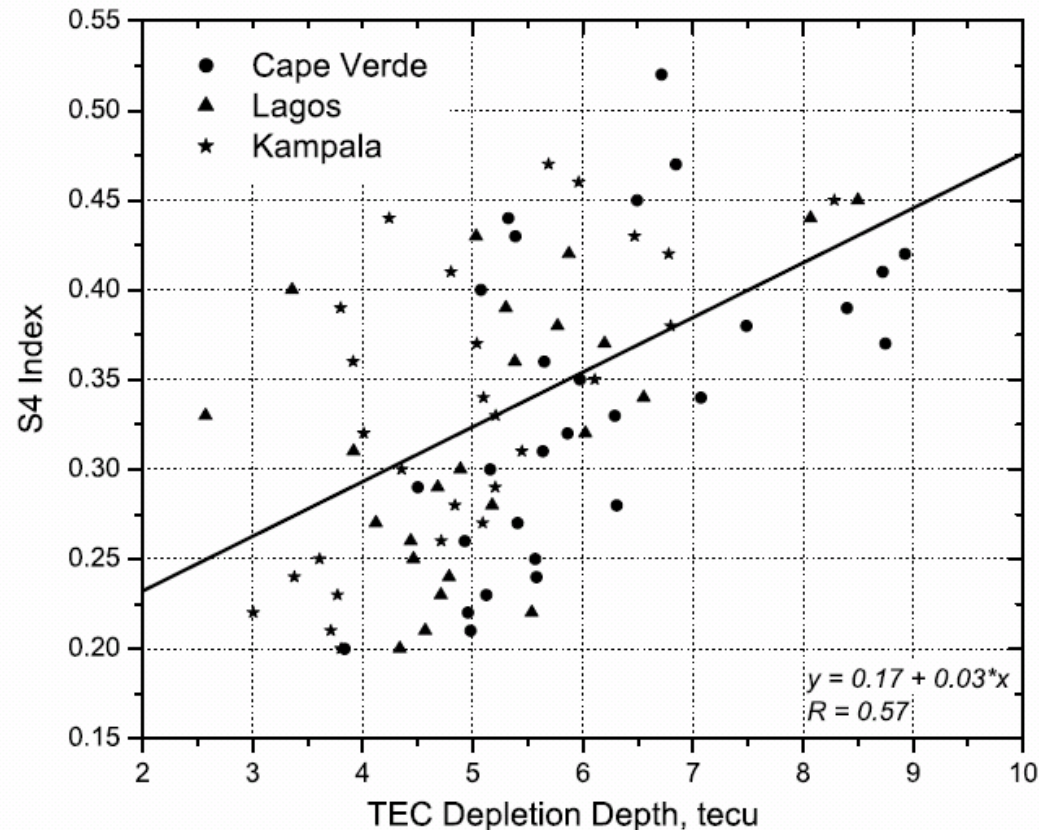
2010



The deepest EPBs mostly follow Tsunoda (1985) climatology, but there is a pronounced increase in the EPB occurrence during June solstice moving west to east.



Relation between the GPS scintillation intensity and TEC depletion depth



Data from three stations Cape Verde, Lagos, and Kampala representing three regions are shown. A best linear fit line is shown with fit coefficients given in the lower right corner. Results show a clear linear dependence between the S4 index and depletion depth, although the spread of the data is rather significant ($R = 0.57$). The ratios between S4 index values and the depletion depth are very close for all three stations. Note that depletions with values smaller than 2 TEC units generally do not produce GPS scintillations.

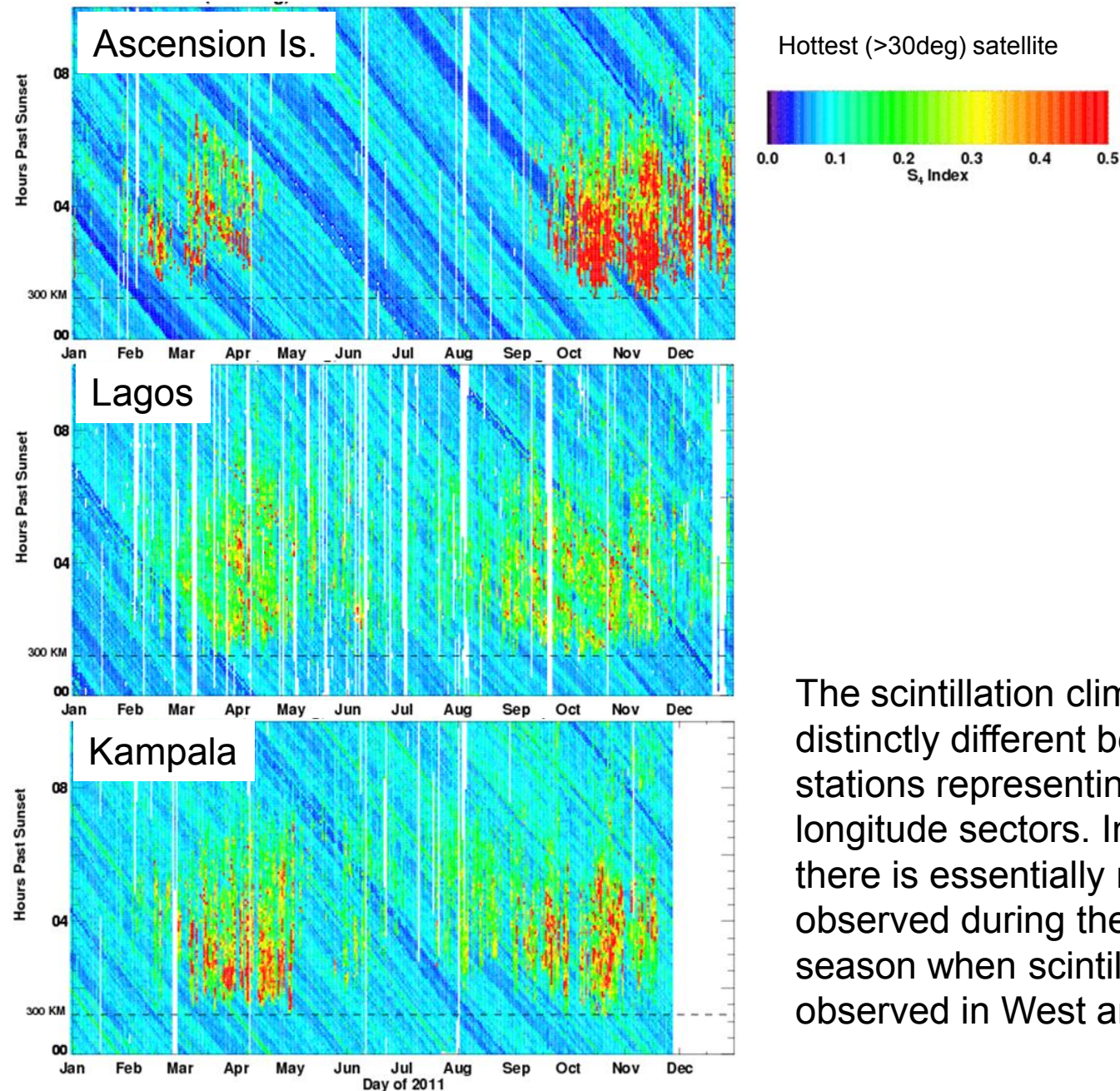


SCINDA sites in 2011





2011 Data from Africa



The scintillation climatology is distinctly different between three stations representing different longitude sectors. In Atlantic region there is essentially no scintillation observed during the boreal summer season when scintillations are still observed in West and East Africa.



Summary and Conclusions



- Our study shows a good correlation between the climatology of EPBs and GPS scintillations in Africa during the solar minimum.
- Seasonal climatology is adequately explained by geometric arguments, i.e., the alignment of the solar terminator and local geomagnetic field (Tsunoda, 1985). The strongest and most frequent GPS scintillations as well as EPBs are occurred during the equinox periods.
- Within the equinox periods, the most intense, longest lasting, and most frequent GPS scintillations and EPBs are observed in Atlantic and West African regions.
- In East Africa the shallower EPBs are observed all year long, even during the summer solstice, when the presence of GPS scintillations appears to be not very significant.
- Outstanding question: What mechanism is responsible for the important transition in the occurrence phenomenology of EPBs and GPS scintillations that occurs between west and east Africa? It seems unlikely that the two regions had significantly different seeding conditions. It will be interesting to look at the role of the 4-cell non-migrating tidal structure.



Summary and Conclusions (cont.)



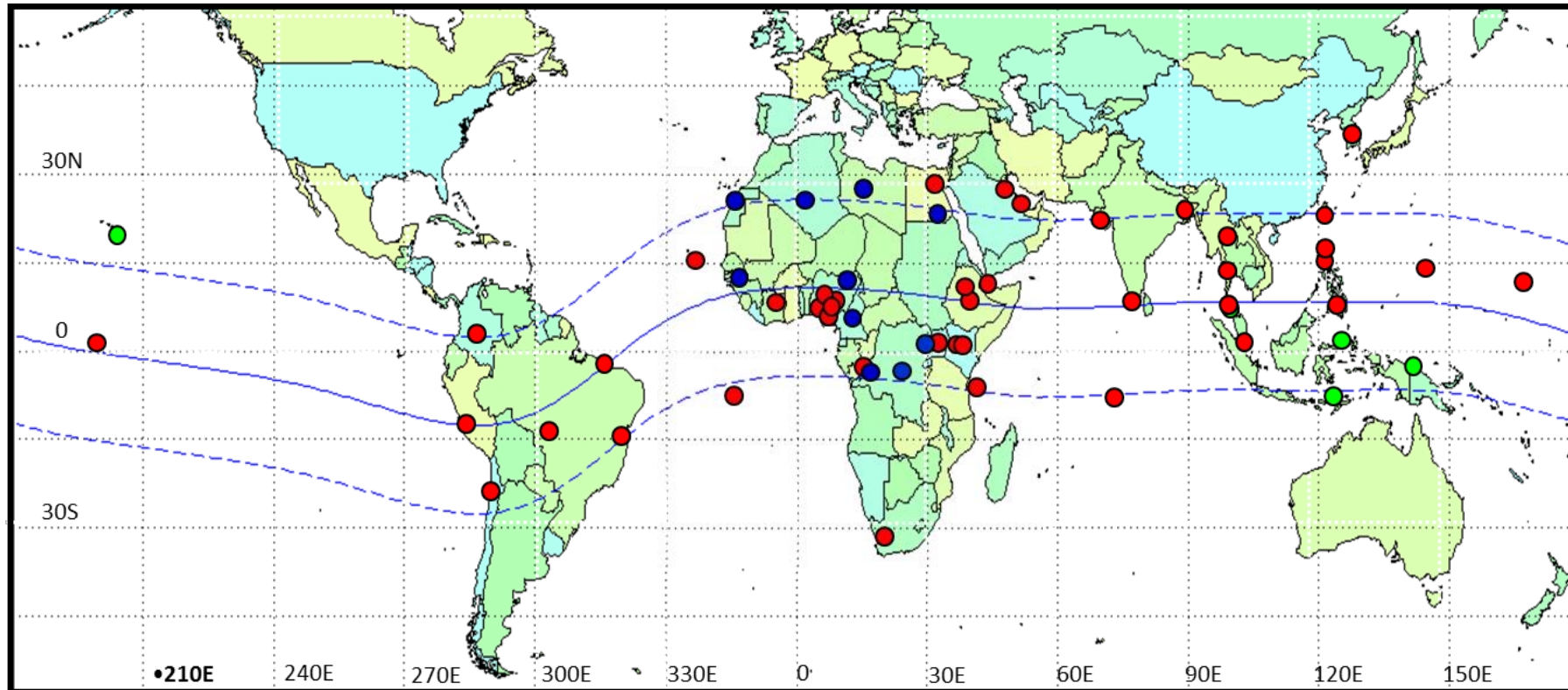
- With the help of our many international partners we are expanding the SCINDA network throughout the African continent. We will be able to study the unique behavior of the equatorial ionosphere over Africa.
- We will ensure global coverage in time for the upcoming solar maximum. However, at least 4-5 more sites are still needed, priority in northern anomaly region.
- We have applied an automated technique to identify EPBs in GPS TEC observations, and found a strong correlation with GPS scintillations. The overall seasonal climatologies of the two phenomena are very similar and consistent with the geometric arguments (i.e., solar terminator alignment with the local geomagnetic field).



SCINDA Ground Stations



Present and anticipated thru 2011



- Existing Sites
- Future ISWI Sites
- Other/collaboration



SCINDA/IHY Workshops



2006 – Cape Verde

- 20 participants representing 7 nations

2007 – Addis, Ethiopia

- ~50 participants from 12 nations at 2007 IHY in Ethiopia

2009 – Livingston, Zambia

- 116 delegates from 27 nations including 79 representing 19 African countries

2010 – Nairobi, Kenya; Bahir Dar, Ethiopia; Cairo, Egypt*

- The beginning of ISWI





SCINDA Africa Network

ISWI Existing Sites (16)



<u>SCINDA Site</u>	<u>Principal Investigator</u>
✓ Abidjan, Ivory Coast	Dr. Olivier Obrou
✓ Addis Ababa, Ethiopia	Dr. Gizaw Mengistu
Akure, Nigeria	Dr. Babatunde Rabi
✓ Bahir Dar, Ethiopia	Dr. Baylie Damtie
Brazzaville, Congo	Dr. Jean Bienvenu Dinga
Cairo, Egypt	Dr. Ayman Mahrous
✓ Ilorin, Nigeria	Dr. Jacob Adeniyi
Ile Ife, Nigeria	Dr. Emmanuel Ariyibi
✓ Kampala, Uganda	Dr. Florence D'ujanga
✓ Lagos, Nigeria	Dr. Larry Amaeshi
✓ (West) Nairobi, Kenya	Dr. Paul Baki
✓ (East) Nairobi, Kenya	Dr. Jared Ndeda
✓ Nsukka, Nigeria	Dr. Bonaventure Okere
✓ Sal, Cape Verde	Mr. Jose Carlos
✓ Zanzibar, Tanzania	Al Amin de Rafara
✓ Sao Tome & Principe	Dr. Rui Fernandes
✓ Hermanus, South Africa	Dr. Pierre Cilliers

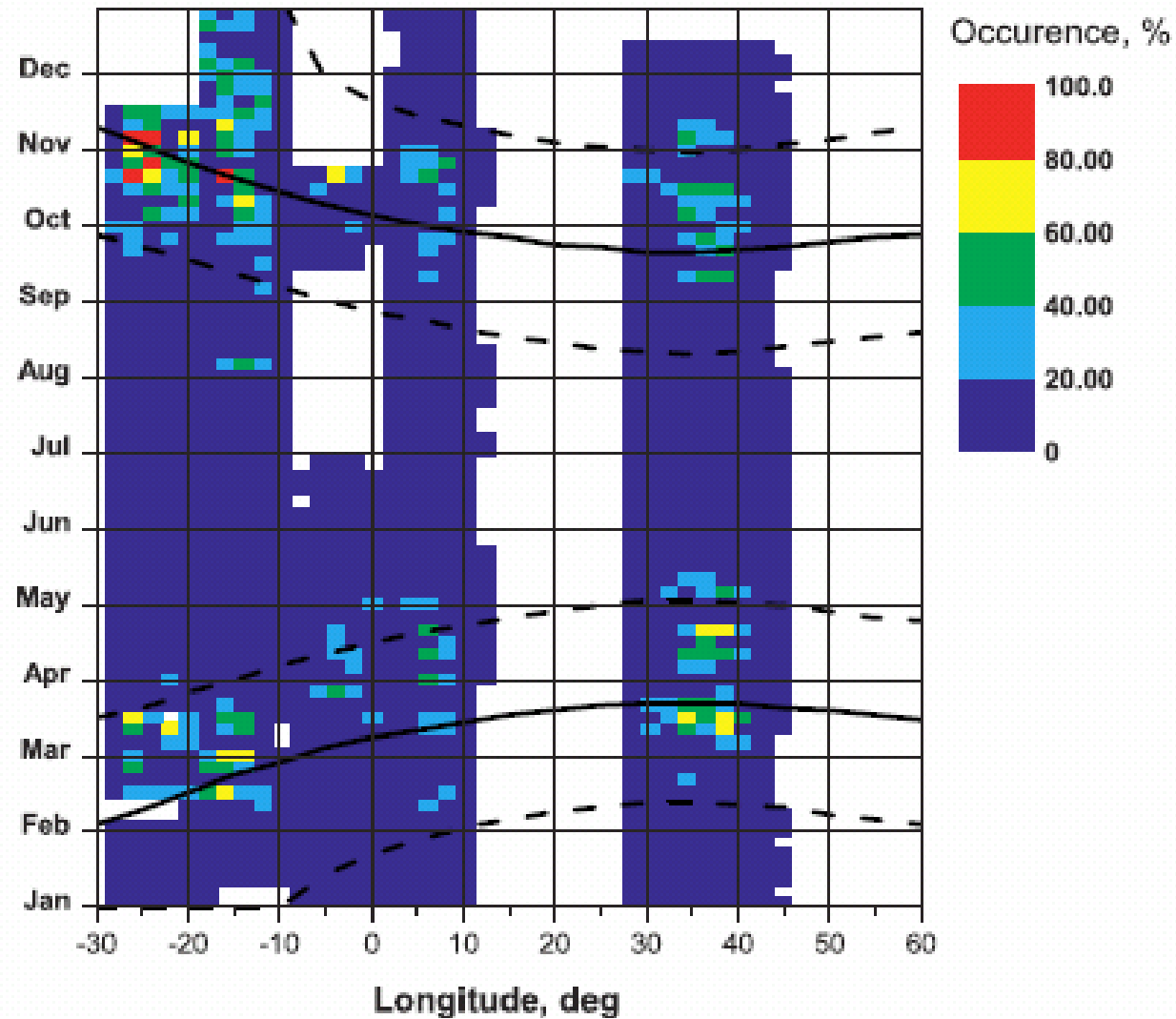
✓ Indicates reporting real-time data



Distribution of GPS scintillations occurrence rate



2010



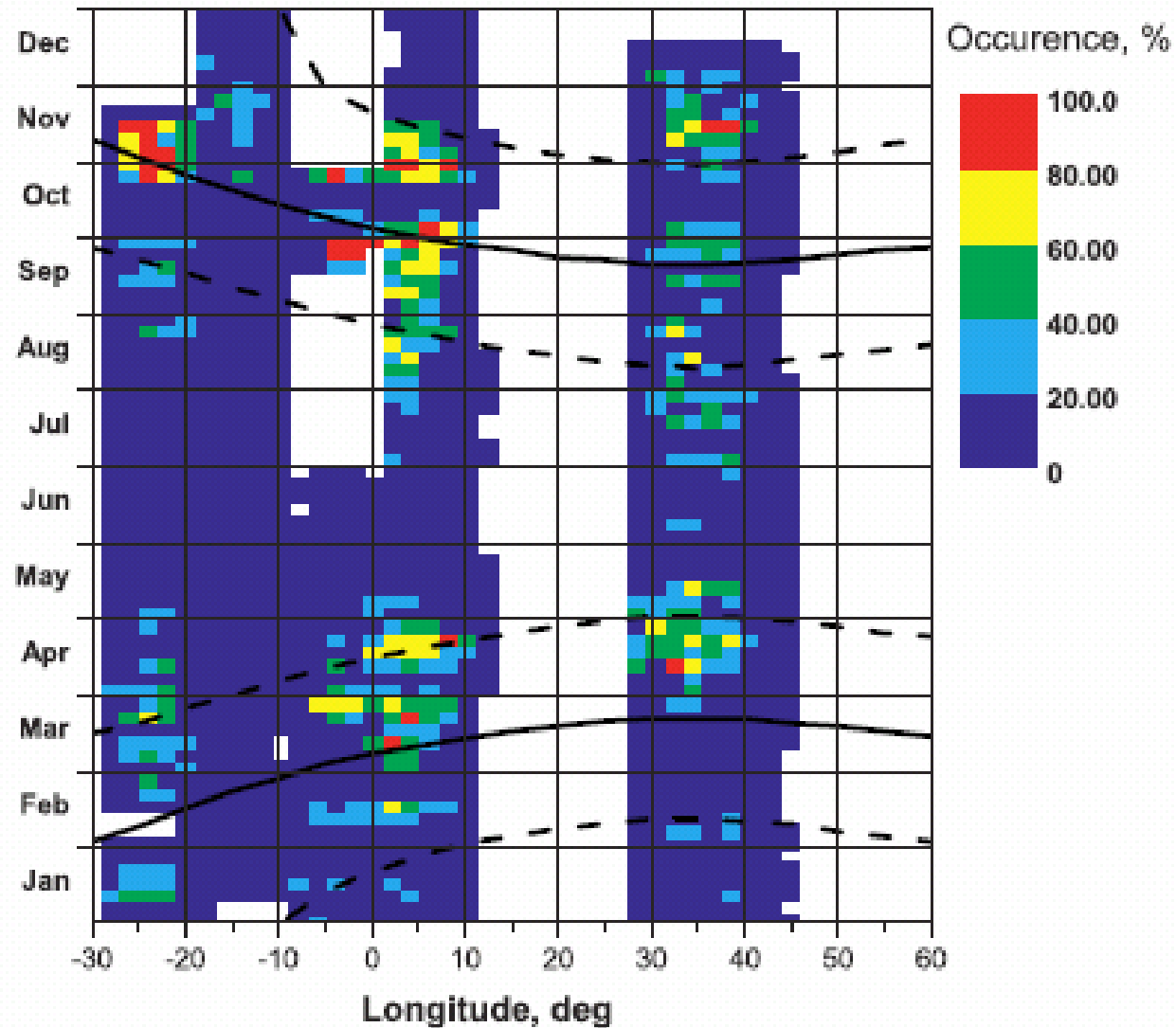
The occurrence rate of S4 scintillations is also in agreement with the solar terminator alignment hypothesis.



Climatology of EPBs occurrence rate



2010



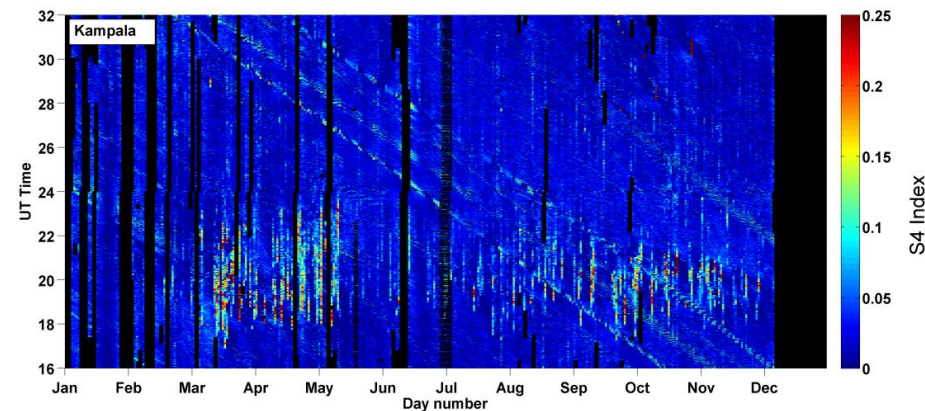
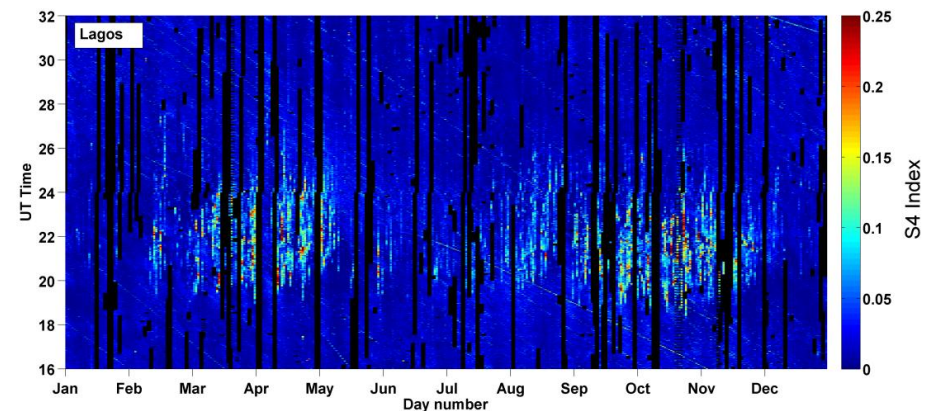
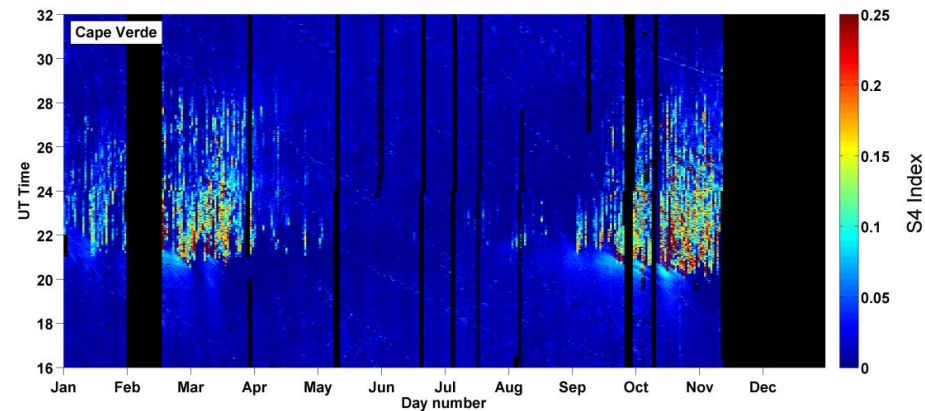
The EPBs occurrence rate overall is consistent with the S4 scintillations occurrence rate. However, in East Africa a significant number of EPBs is observed during the June solstice.



Example of 2010 GPS scintillation data

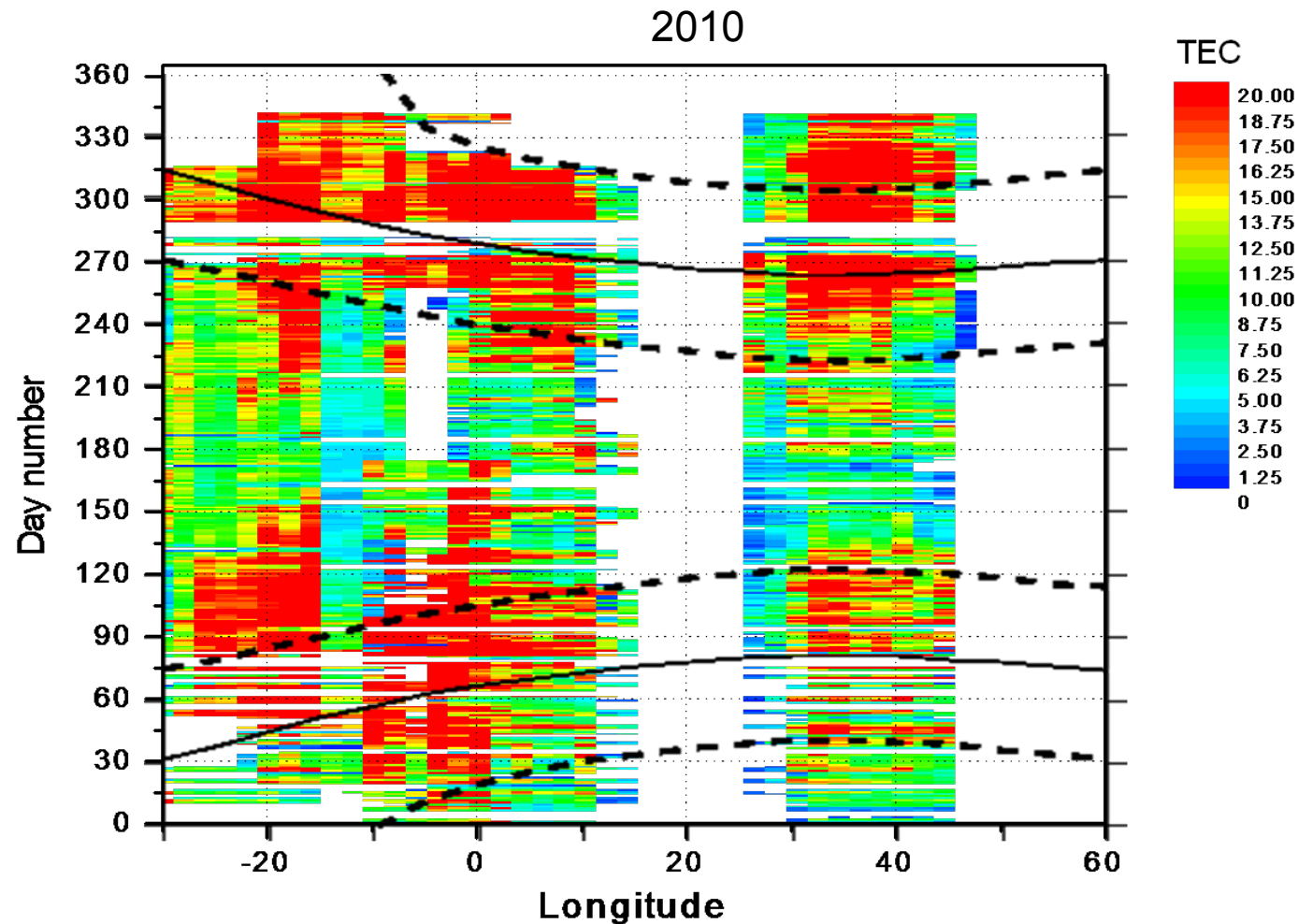


Example of GPS scintillation data for the year 2010 from three regions: Cape Verde, Lagos, and Kampala. The graphs show distribution of the S4 index measurements as function of day of the year and universal time. Black color has been used to indicate missing data.





TEC distribution over Africa



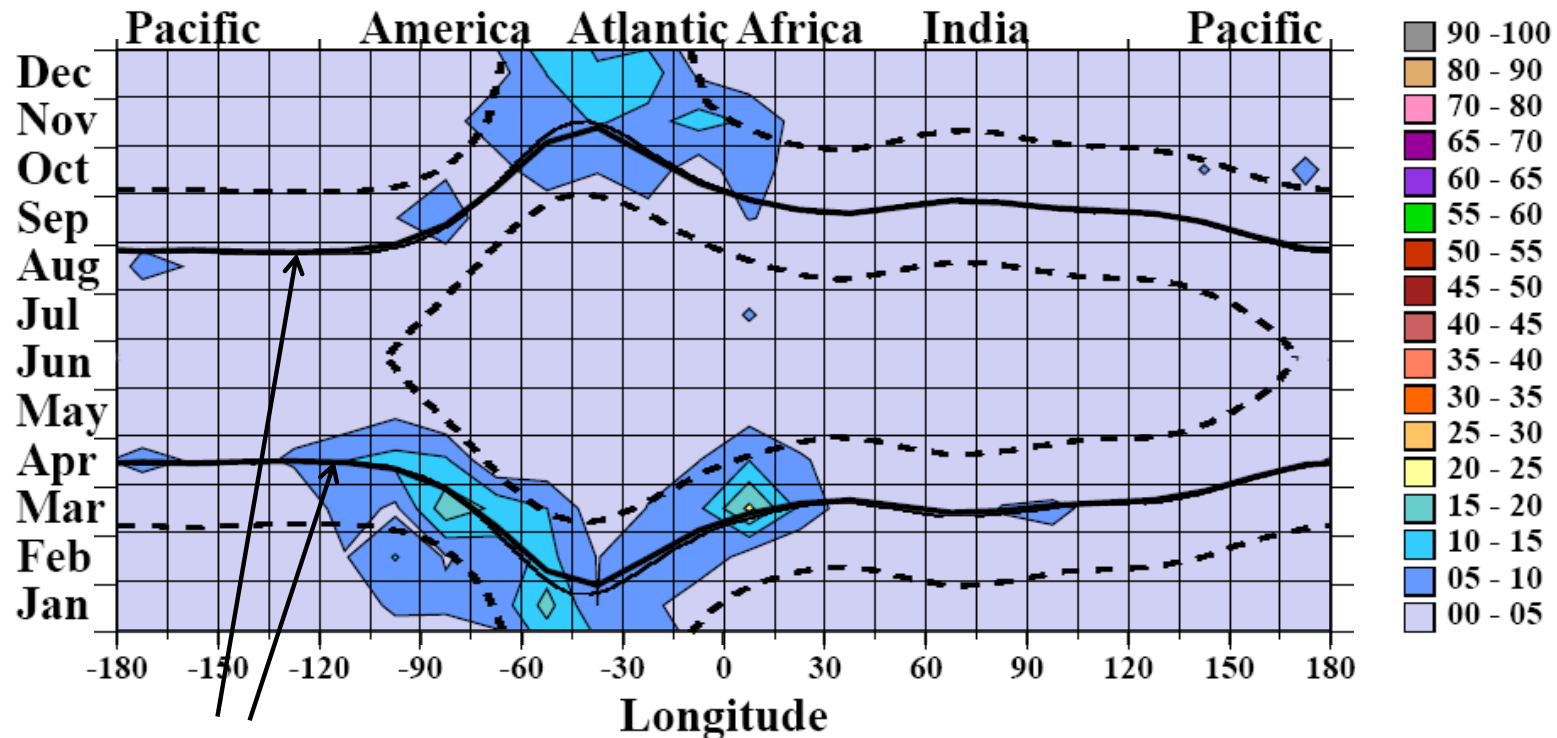
The TEC distribution over Africa for 2010 shows that higher densities are also observed during equinoxes. West Africa appears to have higher TEC during summer solstice period compared to East Africa.



EPB Occurrence Rate from DMSP – Solar Minimum



DMSP EPB Rates 1994 - 1997



Magnetic field aligned
with terminator

L. C. Gentile et al. 2006: A global climatology for equatorial plasma bubbles

- Bubbles seldom rise to DMSP altitude (840 km) during solar minimum
- More (but not all) depletions can be detected from the GPS TEC during solar min.